2017

A Deoxyribozyme Sensor and Isothermal Amplification for Human Sex Determination

Alexandra Smith
University of Central Florida

A DEOXYRIBOZYME SENSOR AND ISOTHERMAL AMPLIFICATION FOR HUMAN SEX DETERMINATION

by

ALEXANDRA SMITH

B.S. North Carolina State University, 2011

A dissertation submitted in partial fulfillment of the requirements

for the degree of Doctor of Philosophy

in the Department of Chemistry

in the College of Science

at the University of Central Florida

Orlando, Florida

Summer Term

2017

Major Professor: Dmitry Kolpashchikov

ABSTRACT

Ribozymes are known to catalyze biochemical reactions and behave like enzymes. They are naturally occurring and have very diverse functions within a cell. After investigating ribozymes that next step was to find if DNA can exhibit the same characteristics since RNA and DNA only differ by a ribose 2'-hydroxyl group. This evolution in curiosity gave rise to artificial DNA enzymes that can catalyze certain reactions and have been created by *in vitro* selection methods. Due to the ability to manipulate and control DNA hybridization, the deoxyribozyme is advantageous to the field of molecular diagnostics. Other hybridization probes like Taqman for PCR (polymerase chain reaction) or a molecular beacon are more conventional methods for molecular diagnostics, but deoxyribozyme-based nucleic acid sensors are overall more sensitive due to their catalytic enhancement of a signal and more selective due to structural design.

When the deoxyribozyme is split into two probes, it is very efficient in identifying a minute difference in sequence compared to the monolith structure. This binary deoxyribozyme sensor (BiDz) has two probes, each containing an analyte binding arm, substrate binding arm, and half of the catalytic core. The monolith structure, known as a catalytic molecular beacon (CMB), contains a hairpin that contains the analyte binding arm in the loop and the substrate binding arms in the stem. The catalytic core is fully intact but deemed inactive due to the substrate binding arms being complimentary to an inhibitory sequence forming the stem. Once the sensor binds the analyte, catalytic core is formed/activated and cleaves a substrate containing

a fluorophore and quencher. When the substrate is cleaved a fluorescent signal is given off denoting the detection of the target DNA.

Deoxyribozyme sensors can be applied to the field of human sex determination by detecting the Amelogenin gene. Found on both sex chromosomes, the Amelogenin gene is the most common marker used for sex determination because it exhibits dimorphism in length and sequence. Sex identification from ancient skeletal remains is crucial to understanding the social structure of our history. When conventional methods, such as metric analysis, are not an option due to the fragmented or prepubescent remains, molecular diagnostics are needed. Amplification of DNA is required to be able to detect the target sequence in human samples. Isothermal loop-mediated amplification (LAMP) is a fast and simple technique that provides ample amounts of amplicon. It is advantageous over PCR because it amplifies at one temperature and no thermal cycler is needed. Two different sensors have been designed to detect the X and Y specific sequences with high selectivity.

From a direct comparison between the CMB and BiDZ, the binary structure has shown to be simpler and less expensive to design, and highly selective toward single base substitutions (SNS). While both sensors contain detection limits in the picomolar range, which is consistent with data published by other research groups, the CMB sensors failed to function at higher temperatures (55^{o}C). BiDz sensors are shown to be superior to the CMB design, particularly when selectivity based analysis is desired. For human sex determination, the binary sensor detected sex specific sequences with great selectivity. The sensor then detected LAMP amplified DNA from male and female teeth after 30 minutes of amplification. Combining a binary

deoxyribozyme sensor and isothermal amplification can provide a new and valuable method for human sex determination.

ACKNOWLEDGMENTS

I would like to thank all members of the Kolpashchikov laboratory for their support over the years of pursing my dissertation. This includes, but is not limited to Martin O'steen, Carlos Ledezma, Nanami Kikuchi, and Maria Stancescu. I would like to acknowledge Dr. Dmitry Kolpashchikov for always offering me his guidance and patience. He was also willing to discuss research and has been a great mentor. From my previous laboratory, where I began my doctoral work, I am very grateful to Dr. Manuel Perez, Dr. Oscar Santiesteban, and Dr. Orielyz Flores. Lastly, I greatly appreciate my committee members: Dr. James Harper, Dr. Andres Campiglia, Dr. Melanie Beazley, and Dr. Laurene Tetard.

TABLE OF CONTENTS

LIST OF FIGURES

LIST OF TABLES

LIST OF ACRONYMS

AMELX	Amelogenin gene on the X chromosome
AMELY	Amelogenin gene on the Y chromosome
BiDZ	Binary deoxyribozyme
CMB	Catalytic molecular beacon
Dz	Deoxyribozyme
F_sub	Fluorogenic substrate
IHP	Instantaneous hybridization probe
LAMP	Isothermal loop-mediated amplification
LOD	Limit of detection
MB	Molecular beacon
PCR	Polymerase chain reaction
SF	Selectivity factor
SNP	Single nucleotide polymorphism

CHAPTER ONE: INTRODUCTION

Deoxyribozyme Sensors

Deoxyribozymes, or DNA enzymes, are catalytic oligodeoxyribonucleotides derived by in *vitro* selection[1,2] and are not produced naturally unlike RNA catalysts (ribozymes). The enzymatic abilities of ribozymes were discovered in the early 1980's[3]. The mechanism of cleavage is not precisely known but it is proposed that the self-cleaving nucleic acids catalyze cleavage of a phosphodiester. More specifically, a nucleophilic attack by a 2' oxygen on an adjacent phosphodiester bond yields a 2'-3' cyclic phosphate and a 5' hydroxyl product as seen in Figure 1[4].

There is a growing number of naturally produce ribozymes being found, including hammerhead, hairpin, and hepatitis delta virus (HDV)-like. Even though DNA and RNA only differ by a 2' hydroxyl group on a ribose and T and U nucleobases, they are used very differently in nature. RNA is a temporary genetic messenger while DNA functions as a long-storage of genetic information. To catalyze a reaction the catalyst must be able to fold into 3D conformations to fully interact with the target molecule. Most of the time DNA is double stranded and cannot acquire a 3D conformation. Yet synthetic single-stranded DNA, very similar to RNA, can fold appropriately and act as a catalyst.

In 1994, Breaker and Joyce, published the first report on a deoxyribozyme that cleaved an RNA monomer within an oligonucleotide (**Figure 2**). They began with a population of 10^{14} DNA strands with 50 random nucleotides. After 5 rounds of selective amplification, the population carried out the cleavage of a target ribonucleoside 3'O-P bond. The sequences were

able to complete the reaction at a rate of 0.2 min^{-1} and have a turnover rate that is 10^5 fold faster than the uncatalyzed reaction. This reaction is also highly dependent on divalent cations. In comparison to proteins, DNA and RNA sequences with catalytic function can be easily identified by Selex (systematic evolution of ligands by exponential enrichment). The most exploited deoxyribozymes are 8-17 and 10-23. Catalytic DNA offers high chemical stability, low cost for synthesis, biocompatibility, and ease of structural prediction and modification[5]. They have shown to be a novel platform for nucleic acid detection due in part to their improved sensitivity because of catalytic amplification of the positive signal. There have been several applications for this sensor due to its high sensitivity and low limits of detection, such as detecting drug-resistant tuberculosis[6], ion detection[7], pH-related studies[8], breast cancer research[9], and biofuel cells[10].

The binary deoxyribozyme sensor proposed herein is comprised of an F-substrate, Dza strand, and Dzb strand. The F substrate contains a fluorophore and quencher conjugated to the opposite ends of the oligomer. Binding to complementary nucleic acids switches the substrate to the elongated conformation and increases its fluorescence. The specificity of nucleic acid recognition is increased by the two components of the probe. Binary probes are more selective than conventional proves because each relatively short hybrid (7-10 nucleotides) is extremely sensitive to single-base mispairings. Each strand contains one end that binds the F-substrate and one end that binds the analyte. When the strands bind the analyte they form a catalytic core that catalyzes the cleavage of the F-substrate, releasing a signal.

Isothermal-loop mediated amplification

DNA amplification is most commonly done with polymerase chain reaction, PCR, but there is a new upcoming technique called LAMP, isothermal-loop mediated amplification. PCR has the ability to amplify very small fragments, accurately, which can be beneficial for molecular diagnostics and was created in 1985 by Kary Mullis[11] (**Figure 3**). This amplification method only needs 2 primers, a forward and backward primer. The most common DNA polymerase used is Taq, which has optimal activity around 72^{o}C. The master mix for the reaction contains DNA primers, nucleotides, buffer, and the enzyme. Then the template of interest is added. For PCR a thermocycler is needed to complete the reaction at three different temperatures. The first step is denaturation of the double stranded DNA template at 95^{o}C. Second, the annealing of the primers to the template strand occurs around 68^{o}C for 30-60 seconds. The third step is the elongation of the new DNA strand via the polymerase. The temperature of this step can vary depending on the polymerase used. Multiple cycles can be run to increase the amount of amplicon desired and based on how much template was used. With 20 cycles of amplification 2^{20} copies of DNA are produced. PCR as the ability to produce short and precise DNA fragments. Also, asymmetric PCR can be performed to produce single stranded DNA (ssDNA) and certain detection methods can only hybridize to ssDNA, such as molecular beacons.

LAMP's advantages come from isothermal conditions and the short amplification time (**Figure 4**). This method of amplification uses 5-7 primers compared to only two for PCR, but can amplify ample amounts of DNA in as short as 15 minutes. The primers usually consist of forward and backward internal primers (FIP/BIP), forward and backward outside primers

(F3/B3), and loop primers (Loop). The FIP/BIP primers contain a complementary sequence that forms a dumbbell shape amplicon and creates another site for elongation. The loop primers can then bind to this region and create an additional site for elongation; with multiple sites of elongation, rapid amplification occurs. Studies have been done with visual detection of the LAMP amplicon due to the byproduct of pyrophosphate. This causes the sample to become cloudy, giving visual recognition that the target was produced. Also a chelating dye can be added to show a color change.

Sex Determination

Identifying the sex of human remains is an important part of the biological profile. When intact skeletons are present sex determination can be done by conventional methods. If fragments or juvenile remains are present the determination of sex can be difficult. Several studies have been done on the pelvis[12], femur and hipbone[13], arm bone[14], sternum[15], scapula[16], and cranium[17] because these bones contain dimorphism, which is the phenotypic differentiation between males and females. If all cranial and pelvic criteria are met, 98% to 100% accuracy in sex estimation can be attained with adult skeletal remains[18]. The overall obstacle lies within partial adult skeletal remains, or juvenile remains.

Sexual dimorphism is apparent only after puberty due to the increased levels of sexual hormones. When metric analysis is used on juvenile skeletal remains, only up to 70% accuracy is achieved. The dentition, which pertains to the development and arrangement of teeth in the mouth, has been found to be the most sexually dimorphic area of the juvenile skeleton[19].

However, sexing juvenile skeletal remains is still challenging because all methods have proven to be population specific, and favor the classification of males over females[20, 21,22].

Through forensic genetics lies the opportunity to determine the sex of juvenile skeletal remains[23,24,25,26]. DNA extracted from adult ancient tissues that are obtained from fragments can be used in the analysis of X and Y-chromosomal DNA. Using polymerase chain reaction (PCR) a single molecule of target DNA can be amplified; hair, bone, or teeth can contain enough DNA to possibly establish a genetic test[27,28]. Methods using markers in the Y chromosome[29], or in both X-chromosomal and Y-chromosomal short tandem repeats (STRs)[30] have been reported, but are not sensitive enough. Also, a successful method using shotgun sequencing has been published, but proves to be too expensive for routine application[31].

Unprecedented archaeological information can be achieved using DNA analysis of ancient human remains. The Amelogenin gene is found on both sex chromosomes and contains sequence and size divergences. AMELX-allele has a size of 2872 bp and is located on the Xp22.1-Xp22.3 region of the X-chromosome, while AMELY-allele has a size of 3272 bp is located on the Yp11.2 region of the Y chromosome[32]. Also, there is a 3-bp deletion on the AMELX-allele compared to the AMELY-allele in a certain region allowing for dimorphism. This gene was originally sequenced by Nakahori et al[33] and is the most widely used target for sexing. A current method done by Alvarez-Sandoval et al uses real-time PCR amplification followed by High Resolution Melting analysis (HRM)[34]. A small fragment (61 and 64 bp) of the AMEL allele is amplified by real-time PCR and the sample remains in the instrument for melting analysis, which greatly decreases the opportunity of contamination. The small fragment was

chosen over a large one to replicate the degradation of ancient DNA and is where the 3-bp deletion is present. Previously published methods have failed due to the highly fragmented DNA samples. Another HRM analysis used SYBR Green as a DNA binding dye and produced differential melting curves[35]. Unfortunately, this dye has the ability to inhibit PCR, promote mispriming, and lacks stability overtime. It also has be known to produce unreliable melting curves due to the "dye redistribution" phenomenon[36].

The most popular method for sex determination is PCR amplification of sequences from the Amelogenin gene, SRY region, or short tandem repeats (STR) sequences of the X and Y chromosome. Once the desired sequence is amplified, gel electrophoresis is ran, and the bands are analyzed. Multiple primers can be used at once for multiplexing and to analyze all three markers at simultaneously; this is known as 'genderplexing"[37].

There is a need for a quicker determination of sex when the researcher is present at the archaeological site. In most countries archaeological findings cannot be removed from the host country. This is an impediment because the laboratory status in that country might not be up to par or have the desired equipment. A deoxyribozyme is an innovative platform that can be used to determine the sex of ancient human remains. Herein we propose a method using a deoxyribozyme sensor for quick and easy sex determination of ancient human remains, along with isothermal loop amplification.

Figures

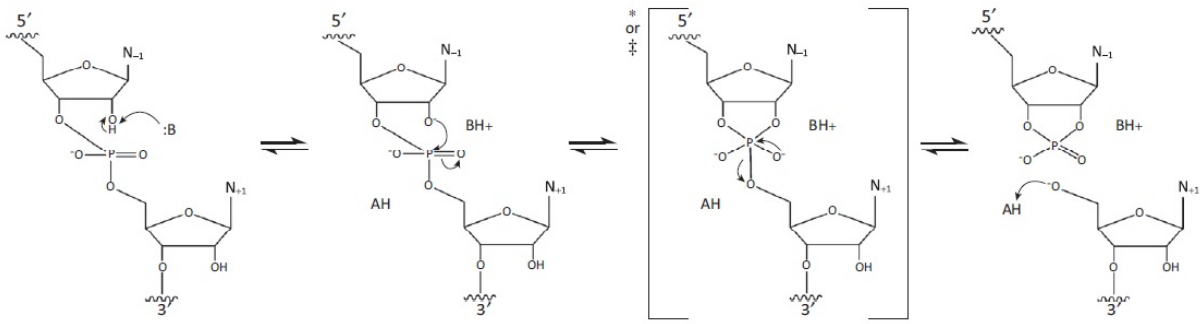

Figure 1. Proposed mechanism of RNA cleavage catalyzed by a deoxyribozyme.

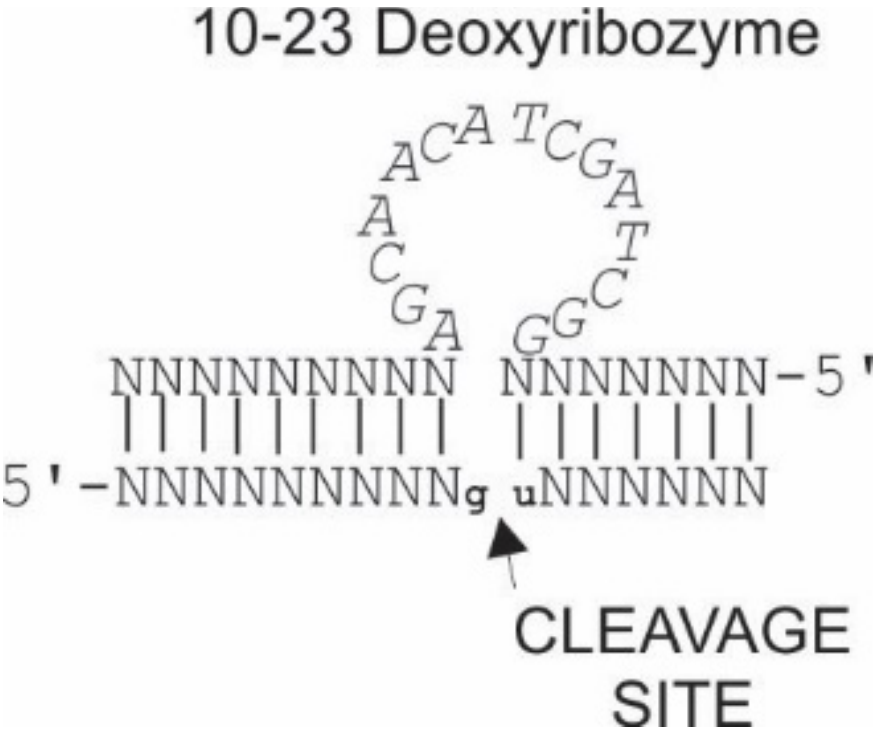

Figure 2. 10-23 Deoxyribozyme. N is a variable DNA sequence. The catalytic core is shown in the loop formation. The lower case letters (g, u) are ribonucleotides where the cleavage occurs.

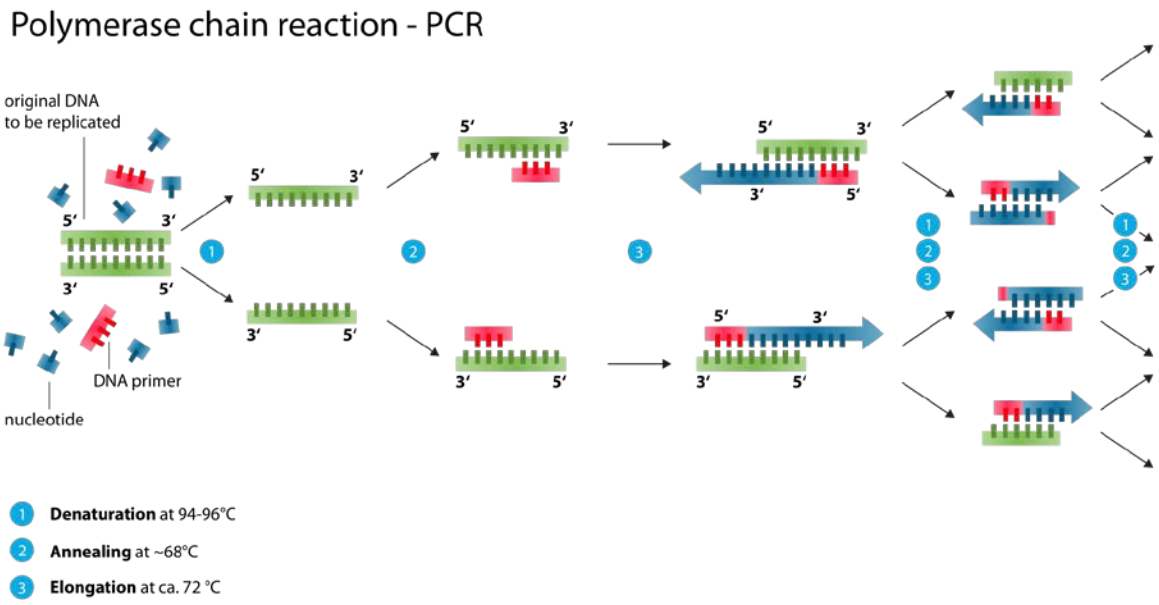

Figure 3. PCR. This image was adopted from https://en.wikipedia.org/wiki/Polymerase_chain_reaction.

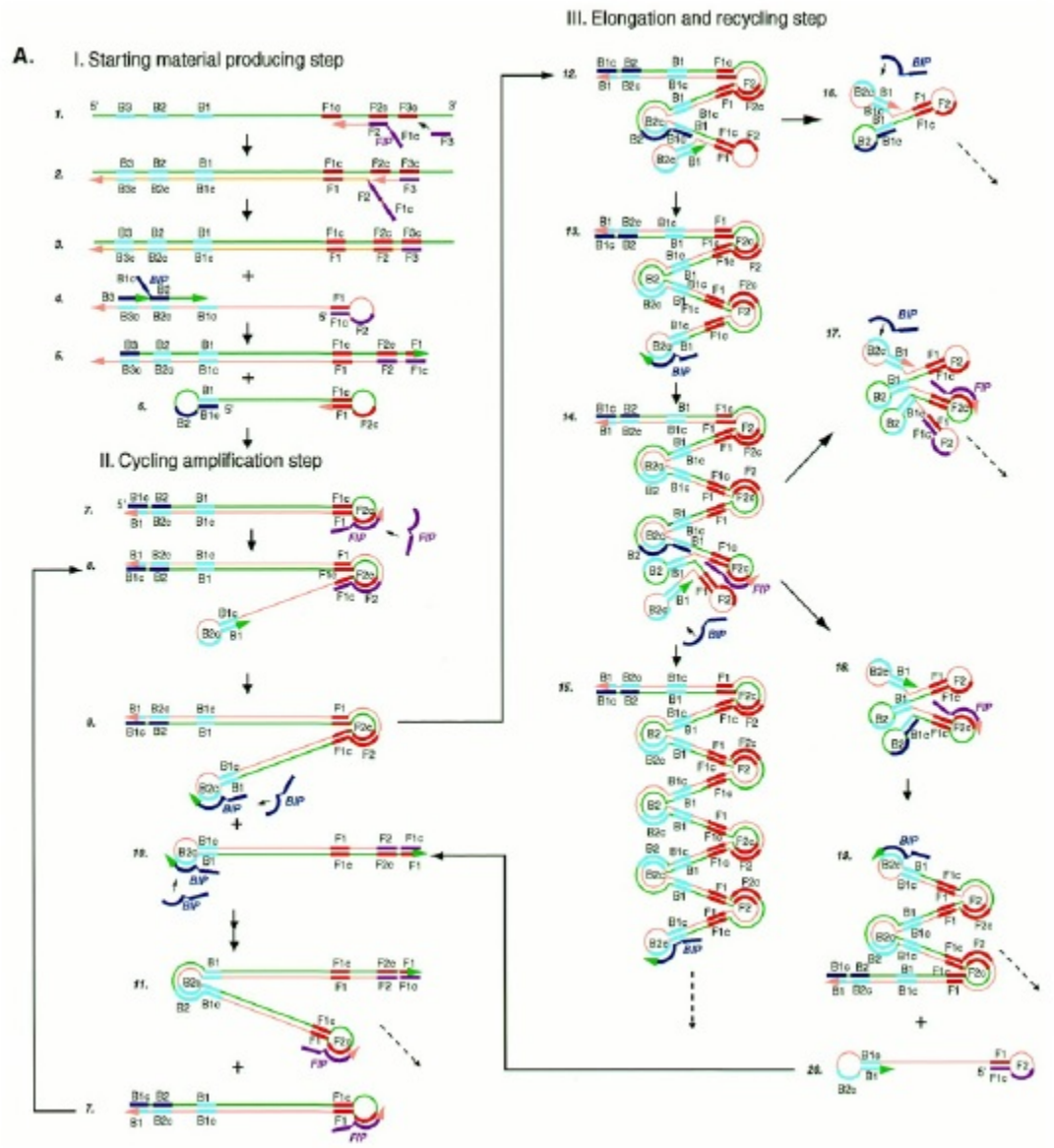

Figure 4. Schematic of LAMP. The first structure formed is a dumbbell shape. With further amplification long zig-zag structures are created that each contain multiple copies of the target sequence. This image was adopted from Zanoli et.al. [38,38b]

CHAPTER TWO: ADVANTAGES OF A BINARY DEOXYRIBOZYME PROBE OVER A CATALYTIC MOLECULAR BEACON

Hybridization probes have been intensively used for nucleic acid analysis in medicine, forensics and fundamental research. Instantaneous hybridization probes (IHPs) enable signaling immediately after binding to a targeted DNA or RNA sequences without the need to isolate the probe-target complex (e.g. by gel electrophoresis). The two most common strategies for IHP design are conformational switches and split approach. A conformational switch changes its conformation and produces signal upon hybridization to a target. Split approach uses two (or more) strands that independently or semi independently bind the target and produce an output signal only if all components associate. Here, we compared the performance of split vs switch designs for deoxyribozyme (Dz) hybridization probes under optimal conditions for each of them. As a split design was represented by binary Dz (BiDz) probes; while catalytic molecular beacon (CMB) probes represented the switch design. It was found that BiDz were significantly more selective than CMBs in recognition of single base substitution at 30^{o}C. CMBs produced high background signal when operated at 55^{o}C. Another major advantage of BiDz over CMB is more straightforward design and simplicity of assay optimization.

Introduction

Hybridization probes for nucleic acid analysis have been used since 1961[39]. The approach takes advantage of selective recognition of a targeted nucleic acid fragment of known sequence by short complementary DNA or RNA probes. The resulting hybrid can be detected by a variety of techniques including blot, fluorescent in situ hybridization or gel electrophoresis. One major

step in the evolution of hybridization probes is the development of instantaneous hybridization probes (IHPs) that can produce a signal (e.g. fluorescence) immediately upon hybridization to the target[40]. IHPs eliminate the need for time-consuming downstream analysis of hybridization mixtures, like gel-based separation of probe-analyte complex from the excess of the unbound probe. Most common designs for IHPs are conformational switches or split (multicomponent design)[41]. Switch IHPs (e.g. molecular beacon probes[42] and their variations[42b, 43]) change conformations upon hybridization to the target sequence and produce a signal. Split probes (e.g. adjacent hybridization probes[44]) consist of several parts, which produce output signal upon hybridization to the analyzed sequence[45]. In this study we directly compare the performance of the two designs.

One of the most promising IHPs are deoxyribozyme (Dz)-based probes, for which both the switch[46] and the split designs[5] were explored earlier. Dz's are short catalytic DNA sequences derived by in vitro selection[47]. Most of the Dz's used in analytical applications catalyze cleavage of RNA phosphodiester bonds[48], which can be conveniently converted to a fluorescent response, as shown in Scheme 1A: Dz binds a fluorophore- and a quencher-labeled DNA/RNA chimera substrate and cleaves the internal RNA phosphodiester bond (red in **Figure 5A**), thus separating the fluorophore from the quencher. We and others take advantage of RNA-cleaving Dz in developing IHPs[49]. One major advantage of Dz probes over other IHP (e.g. MB probes) is improved sensitivity and reduced limits of detection (LOD) due to the catalytic amplification of the output signal: one analyte bound to a Dz probe triggers cleavage of multiple **F-sub** molecules (**Figure 5A**). Another advantage is that expensive **F-sub** can be used for multiple analytes, given that Dza and Dzb are adjusted to each new analyte sequence, which reduces the cost if multiple

sequenced need to be analyzed. Two alternative designs of Dz probes for nucleic acid analysis have been explored so far: allosteric switch named in the original publication 'catalytic molecular beacon[46] (CMB), and split design, named binary Dz probe (BiDz)[5] (**Figure 5B** and **C**, respectively).

The CMB design uses a monolith construct, in which the Dz catalytic site is inhibited by hybridization within the complementary sequence: the strategy akin to the intrasteric regulation in proteins[50]. Binding of the complementary DNA/RNA analyte reduces the inhibition and releases the catalytic core, which cleaves fluorogenic substrate (F_sub) and produces the detectable signal[46]. In the split strategy, the parent Dz is divided into two parts with analyte binding arms appended to each part (Dza and Dzb in **Figure 5C**). In the presence of a complementary analyte, the two strands assemble the catalytic site, which cleaves F_sub followed by increase in fluorescence. In this study we compared the two designs in terms of selectivity (the ability to differentiate analytes with a signal nucleotide substitution (SNS)), limit of detection (LOD) and optimization simplicity. We assume that any two sensors can be compered using the aforementioned parameters demonstrated by the sensor under near optimal conditions. Up to the best of our knowledge, this is the first direct experimental comparison of the two designs.

The following analytes were used in this study (**Table 1**): T1 represents a fragment of the TWIST1 gene coding for a transcription factor involved in cancer development[51]. The second targets A1, represent the sequence from amelogenin gene and is used as a genetic marker for sex determination[52]. The choice of the two practically significant but otherwise random targets was

made to ensure a more general applicability of the conclusions made in this study. To test the probes selectivity, a SNS was introduced into both T1 and A1 to make T2 and A2, respectively.

We designed two variants of CMB and BiDz probes based on the most catalytically efficient deoxyribozyme 10-23[49f, 53] one made to recognize the analyte at 30ºC, another optimal for 55ºC. Lower temperature was chosen to compare our results with the earlier reported data collected under similar conditions[42-43] and because of the importance of point-of-care diagnostic assays operating at near room temperature[54]. Both switch and split designs were accomplished according to the strategies reported earlier for optimal performance of each design under given conditions.

Materials and Methods

DNAse/RNAse free water was purchased from Fisher Scientific, Inc. (Pittsburgh, PA, USA) and used for all buffers and for the stock solutions of oligonucleotides. . Oligonucleotides were custom made by Integrated DNA Technologies, Inc. (Coralville, IA, USA) and by TriLink BioTechnologies, Inc. (San Diego, CA, USA). Oligonucleotide structures were calculated using the mfold web server by the RNA Institute (University at Albany)[55]. In all structures, nucleotides outlined in green are complimentary to the analyte, blue are complimentary to the **F_sub**, and red signifies the catalytic core. Reaction buffer used in the following experiments consisted of 50 mM hepes, 50 mM MgCl2, 20 mM KCl, 120 mM NaCl, 0.03% Triton X-100, 1% DMSO. Fluorescent spectra were measured with a Perkin-Elmer (San Jose, CA, USA) LS-55 luminescence spectrometer with a Hamamatsu xenon lamp. Experiments were performed at an

excitation wavelength of 485 nm and emission was monitored from 500 to 550 nm; data were processed by using Microsoft Excel.

Sensitivity Experiments

F sub (200 nM) and sensor strands (CMB or Dza and Dzb) (5 nM) were incubated with various concentrations of analytes in the reaction buffer (50 mM HEPES, pH7.4, 50 mM MgCl2, 20 mM KCL, 120 mM NaCl, 0.03% Triton X-100, 1% DMSO). After 1 or 3 hour of incubation at 30ºC or 55ºC the fluorescence of the samples was measured at 517 nM at room temperature. Control samples contained only F sub and sensor strands. The average values of three independent experiments were plotted as a function of analyte concentration.

Selectivity Experiments

F_sub (200 nM) and sensor strands (5 nM) were incubated in the presence of either the matched analyte or single-based substituted analyte (1 nM for A1/A2 or 5 nM for T1/T2). The control sample did not contain any analyte. After 1 hr of incubation at 30ºC or 55ºC the sample fluorescence was measured at 517 nM (λ_{ex} = 485 nm) at room temperature. These measurements were used to calculate the selectivity factors.

Results and Discussion

We tested three CMB constructs (**Table 1**) with different lengths of the inhibitory fragment, which was progressively elongated to suppress CMB response in the absence of T1 analyte. The three CMB probes were also HPLC purified prior testing to reduce the undesired background response. The best CMB, named CMB_TWIST_30 (**Figure 6 A**) produced signal-to-background ratio (S/B) of ~ 3 (1 hr of incubation, 5 nM analyte). The structure and limit of

detection for this sensor are shown in **Figure 7**. The results for other two CMB constructs are included in **Figures 8** and **9**.

Importantly, the differentiation of single base mismatched analyte T2 was not impressive (**Figure 6A**, bar graph), which was quantified using the selectivity factor (SF, **Table 2**). This data correlates well with earlier observations that CMB constructs can unambiguously discriminate only analytes with two mismatched bases, but not with SNS[46, 49a]. In contrast, BiDz probe demonstrated near perfect selectivity towards T2 analyte (**Figure 6B**). Importantly, no HPLC purification of Dza_ TWIST_30 and Dzb_ TWIST_30 was needed, since contamination with shorter DNA products arose form incomplete DNA synthesis do not contribute to the elevated background as in the case of CMB design. Furthermore, the low background for BiDz can be achieved by optimizing the concentrations of Dza and Dzb strands. Therefore, we achieved near-optimal performance of the initially designed Dza_TWIST_30 and Dzb_TWIST_30 simply by reducing their concentrations to 5 nM (**Figure 10**). Similar probe design and optimizations were performed for CMB and BiDz probes that recognize A1 and A2 analytes. The obtained results demonstrate similar trend in terms of probe selectivity and LODs (**Table 2** and **Figures 11, 12**).

It was shown earlier that BiDz based on deoxyribozyme 10-23 has higher catalytic rates and lower LODs at elevated temperatures[49f]. We, therefore, designed CMB and BiDz probes for the detection of T1 and A1 analytes at 55^{o}C. First, substrate-binding arms were elongated by 3 nucleotides each to enable binding of F_sub by the Dz constructs even at 55^{o}C. **Figure 13A** demonstrates the design and selectivity data for one of the CMB construct, CMB_ AMELY_55.

Importantly, the probe experienced leakage, as reflected by the high background (**Figure 13B**, "no analyte" bar). We attempted to redesign the CMB construct to increase the stability of the folded structure in the absence of the analyte, but without success (**Figure 14 and 15**). As a result of the high background, the signal for both the matched and mismatched analytes was only slightly above the background; the differentiation between fully matched A1 and SNS containing A2 was not observed (**Figure 13A**, bar graph, **Table 1**). The BiDz probe, on the other hand, demonstrated high analyte-dependent turn-on ratio (S/B), as well as impressive selectivity (see DF in **Table 2**). The LOD of 8 pM was achieved after 3 hrs of incubation, which is consistent with the previously reported data[49f] (**Figure 16**). The lowest LOD for CMB was about 7-fold higher than the best value for BiDz. Similar design, optimization experiments and results were obtained for T1 and T2 analytes and their corresponding sensors (**Table 1** and **Figure 17, 18**).

Conclusion

Among the enzyme-free approaches, switch probes have received significant attention for the last 20 years and now dominate in majority of applications or the original development[40, 42-43]. For example, allosteric switch probes based on spinach aptamer have been reported recently[56]. In parallel, binary and multicomponent probes have been developed[6, 44a, 44b, 57]. In this study, we directly compared the two designs using Dz probes, one of the most promising IHPs. Our main conclusions are the following. (i) Split design is simpler and less expensive to optimize. (ii) Switch probes fail to work at 55^{o}C. (iii) Split probes have significantly high selectivity toward single base substitutions. (iv) The detection limits for both design are comparable and consistent with the data published by different research groups. We conclude that our results taken together

with the prior observations strongly suggest that split probes are advantageous to switch hybridization probes especially if SNS differentiation is required.

Figures and Tables

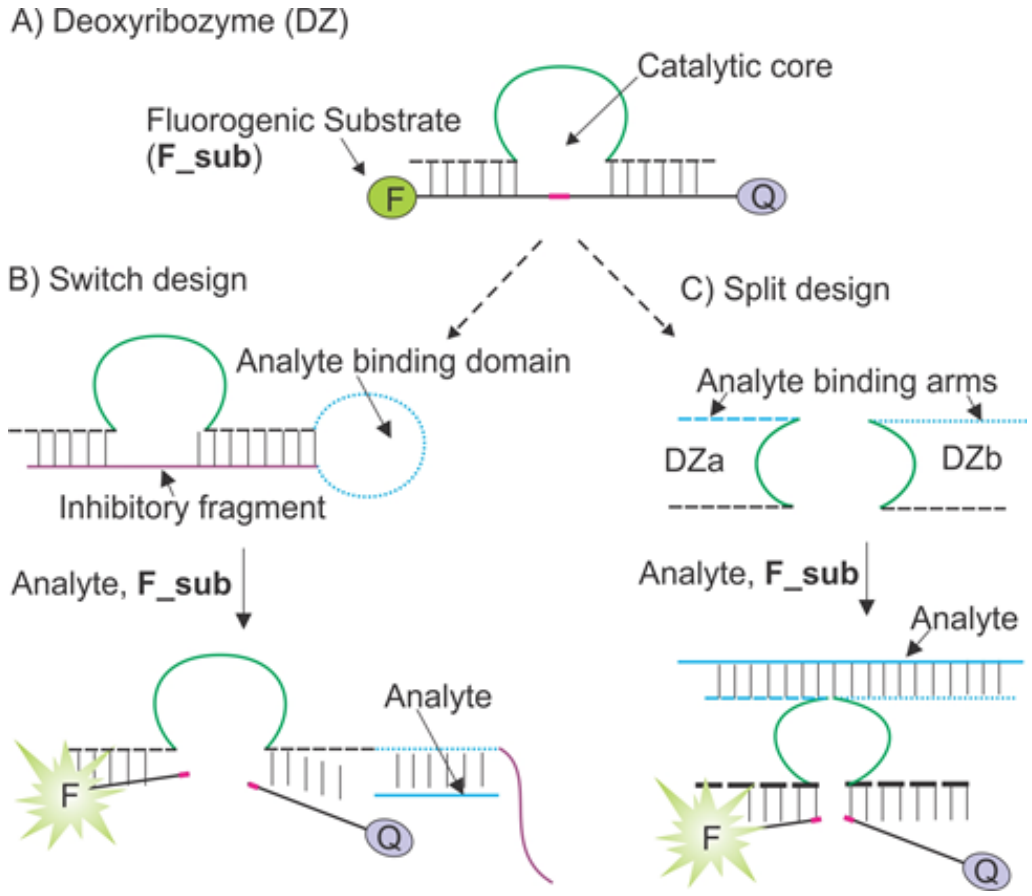

Figure 5**.** Design of deoxyribozyme (Dz) probes that produce fluorescent signal upon hybridization to specific nucleic acid analytes. A) Parent RNA-cleaving Dz can cleave a fluorophore- and quencher-labelled substrate (**F_sub**), thus producing high fluorescence. B) Switch design for Dz hybridization probe: the catalytic core and/or substrate binding arms of Dz are inactivated by binding to the 'inhibitory fragment'; hybridization of the analyte to the analyte binding domain releases the substrate binding arms of the Dz construct and enables cleavage of **F_sub**; C) Split design: two DNA strands Dza and Dzb hybridize to the analyte sequence and form catalytically active Dz, which cleaves **F_sub**.

Table 1. Oligonucleotides

Name (comments)	Sequence 5'->3'	Purification
F_sub	AAG GTT^{FAM} TCC TC**g u**CCC TGG GCA-BHQ1	HPLC
T1 (TWIST)	TAG TGG GAC GCG GAC ATG GAC CAG GCC CCC TCC ATC CTC CA**G** ACC GAG AAG GCG TAG CTG AGC CGC TCG TGA GCC A CA TAG CTG CA	SD
T2 (TWIST mutant)	TAG TGG GAC GCG GAC ATG GAC CAG GCC CCC TCC ATC CTC CA**A** ACC GAG AAG GCG TAG CTG AGC CGC TCG TGA GCC ACA TAG CTG CA	SD
CMB_TWIST_30	GTT TCC TCG AGC GGC TCA GCT ACG CCT TCT CGG TCT GGA GGA TGG AGT TTT TCC AGG GA *G GCT AGC TAC AAC GA* GAG GAA A C	HPLC
CMB_TWIST_A_30	CG AG CGG CTC AGC TAC GCC TTC TCG GTC TGG AGG ATG GAG TTT TT CCA GGG A *GG CTA GCT A CAA CGA* GAGGAAAC	SD
CMB_TWIST_B-30	GTT TCC TTC TCG GTC TGG AGGA TTTTT CCA GGG A *GG CTA GCT A CAA CGA* GAG GAA AC	HPLC
DZa_TWIST_30	CGA GCG GCT CAG CTA CGC CT *A CAA CGA* GAG GAA AC	SD
DZb_TWIST_30	CCA GGG A *GG CTA GCT* TCT CGG T**C**T GGA	SD
DZa_TWIST_55	G TGG CTC A CGA GCG GCT CAG CTA CGC CT *ACA ACG A* GAG GAA AC CTT	SD
DZb_TWIST_55	TGC CCA GGG A *GG CTA GCT* TCT CGG TCT GGA GGA	SD
CMB_TWIST_55	CGT TG T AGCTAG CT TCT CGG TCT GGA GGA TG TTTTT TGC CCA GGG A *GG CTA GCT A CAA CGA* GAG GAA ACC TT	HPLC
A1 (AMELY)	CTC CAG CAC CCT CCT GCC T**G**A CCA TTC GGA TTG ACT CTT TCC TCC TAA ATA TGG CTG TAA GTT TAT TCA T	SD
A2 (AMELY $_{mut}$)	CTC CAG CAC CCT CCT GCC T**A**A CCA TTC GGA TTG ACT CTT TCC TCC TAA ATA TGG CTG TAA GTT TAT TCA T	SD
CMB_AMELY_55	GCT AGC CTC CCT GGA GTC AAT CCG AAT GGT CAG GCA GGA GTT TTT TGC CAG GGA *GGC TAG CTA CAA C GA* GAG GAA ACC TT	HPLC
CMB_AMELY_A-55	AGG TTT CCT CTC GAG TCA ATC CGA ATG GTC AGG CAG GAG TTTTT TGC CAG GGA *GGC TAG CTA CAA CGA* GAG GAA ACC TT	HPLC
CMB_AMELY_B-55	AAG GTT TCC TCT CGT TGT AGC TAG CCT CCC TGG AGT CAA TCC GAA TGG TCA GGC AGG AG TTTTT TGC CAG GGA *GG CTA GCT A CAA CGA* GAG GAA ACC TT	HPLC
DZa_AMELY_55	TGC CAG GGA *GG CTA GCT* GAA TGG T**C**A GGC AGG	SD
DZb_AMELY_55	TAG GAG GAA AGA GTC AAT CC *A CAA CGA* GAG GAA ACC TT	SD
DZa_AMELY_30	GAG GAA AGA GTC AAT CCG *A CAA CGA* GAGGAAAC	SD
DZb_AMELY_30	CCA GGG A *GG CTA GCT* AAT GGT CAG GC	SD
CMB_AMELY_30	GTT TCC TCG AAT GGT CAG GCA GTT TTT CCA GGG A GG CTA GCT A CAA CGA GAG GAA AC	HPLC

[a]BHQ-1, Black Hole Quencher1; F_Sub binding arms are underlined; [b]The SNP sites are bold underlined, nucleotides part of the catalytic core are in italic; [c]SD, standard desalting; [d]Ribonucleotides are in low case

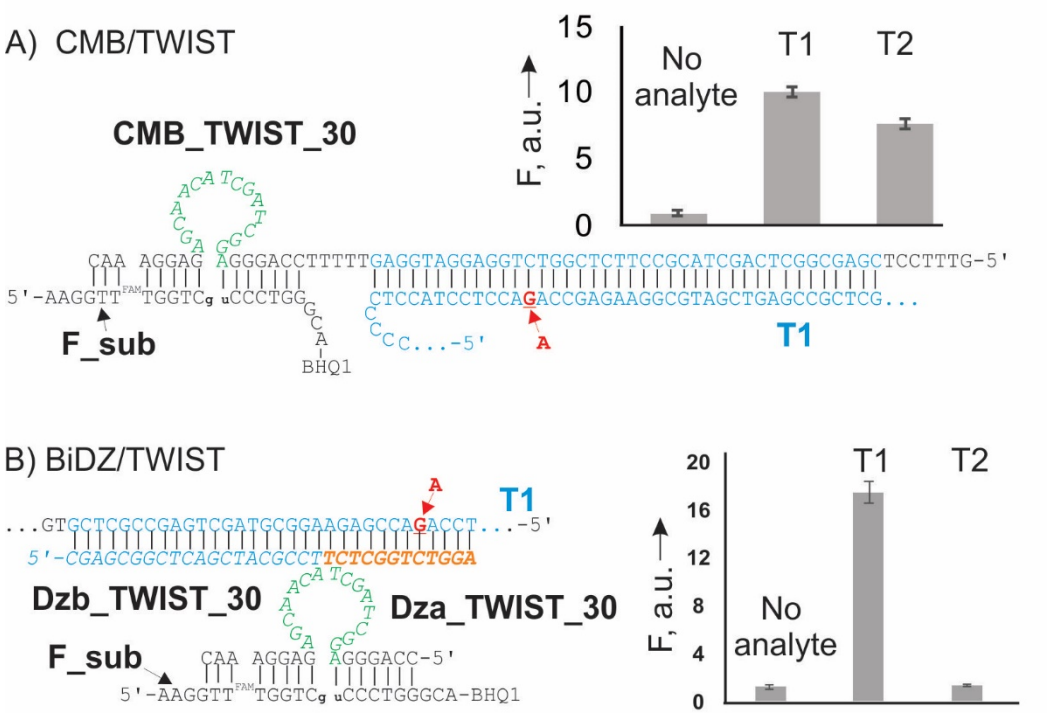

Figure 6. Predicted structures of the probe-analyte complexes and selectivity data for CMB (A) and BiDZ (B) recognizing **T1** analyte at 30ºC. For structures: catalytic core nucleotides are in italic; single base substitution site is bold underlined; ribonucleotides are in low case. For right panels: all samples contained 200 nM **F_sub** and either 5 nM **CMB_TWIST_30** or 5 nM each **Dza_TWIST_30** and **Dza_TWIST_30** in the reaction buffer: 50 mM HEPES, 50 mM $MgCl_2$, 20 mM KCl, 120 mM NaCl, 0.03% Triton X-100, 1% DMSO. Samples **T1** and **T2** contained 5 nM of fully complementary **T1** and 5 nM single base mismatched **T2** analytes, respectively (for full sequences see Table S1). Fluorescence intensity at 517 nm (emission at 485 nm) was measured after 1 hr of incubation. The data are average values of 3 independent experiments.

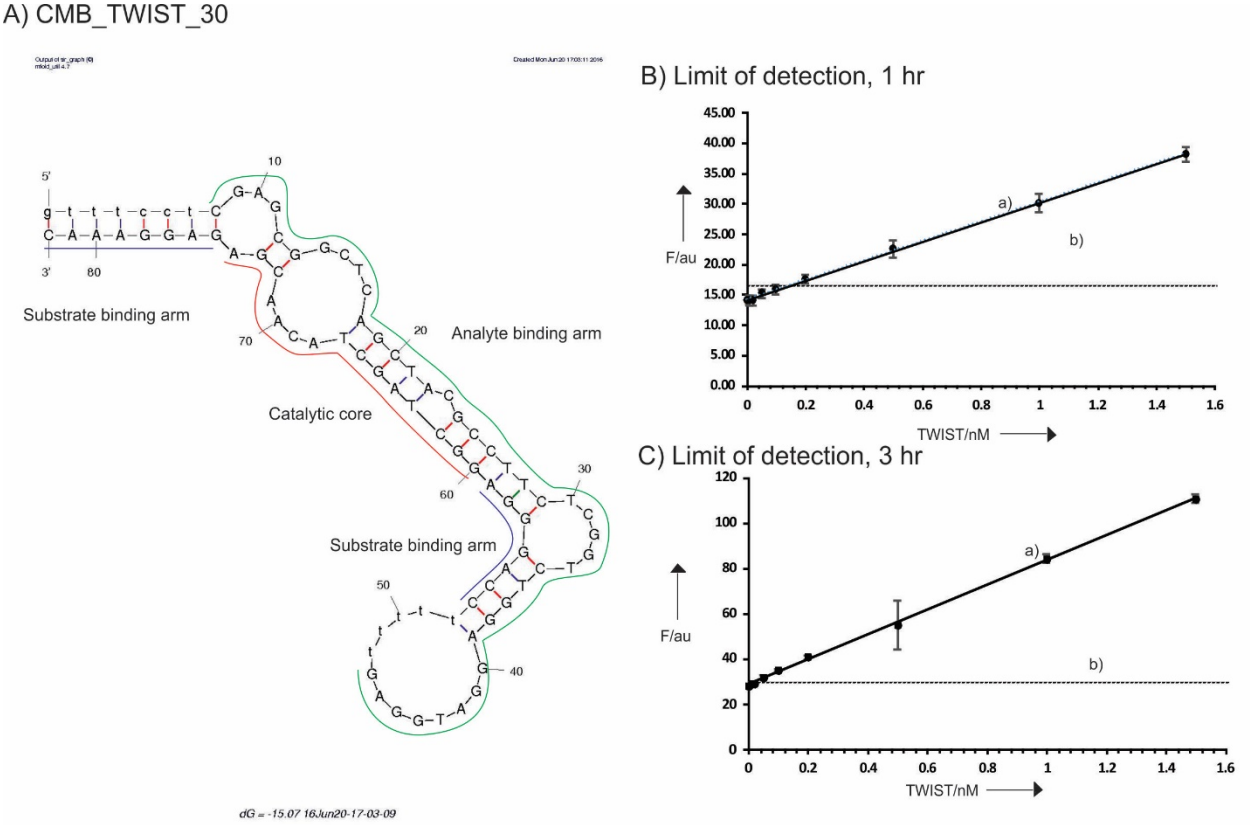

Figure 7. **CMB_TWIST_30** structure and performance. A) Mfold calculated structure. Conditions for folding were 30ºC, 90 mM Mg^{2+}, and 50 mM Na^{+}. The structure was traced in green, blue and red to denote the analyte binding arm, substrate binding arm, and catalytic core, respectively. Samples contained 200 nM **F_sub**, 5 nM CMB, and various amounts of analyte (0 nM -0.2 nM) in reaction buffer. After 1 and 3 hrs incubation at 30ºC in a water bath the fluorescence was measured. C) Limit of detection after 1 hr reaction was 132 pM (a) and the threshold (b) was calculated as three standard deviations above the control (0 nM analyte). D) Limit of detection for 3 hrs hybridization was 11 pM (a) and the threshold (b) was calculated as three standard deviations above the control (0 nM **T1** analyte).

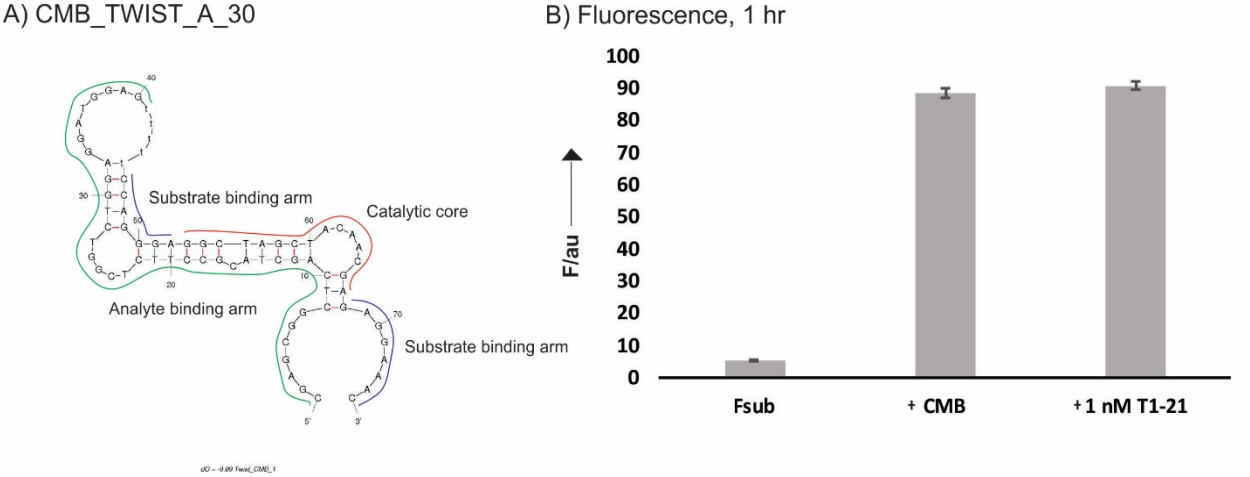

Figure 8**. CMB_TWIST_A_30** structure and performance for reduced background signal. A) Mfold calculated structure that contains long binding arms and secondary structure to prevent leakage, cleavage of substrate with no analyte present. Conditions for folding were 30ºC, 50 mM Mg^{2+}, and 90 mM Na^{+}. The structure was traced in green, blue and red to denote the analyte binding arm, substrate binding arm, and catalytic core, respectively. B) Fluorescent performance of sensor. 'Fsub' control contained 200 nM of **F_sub** in reaction buffer. '+CMB' control sample consisted of 200 nM **F_sub** and 5 nM **CMB_TWIST_A_30**. Sample '+1 nM T1-21' contained the same components as the +CMB control with the addition of 1 nM of **T1-21** analyte. The samples were incubated at 30ºC for 1 hr and measured.

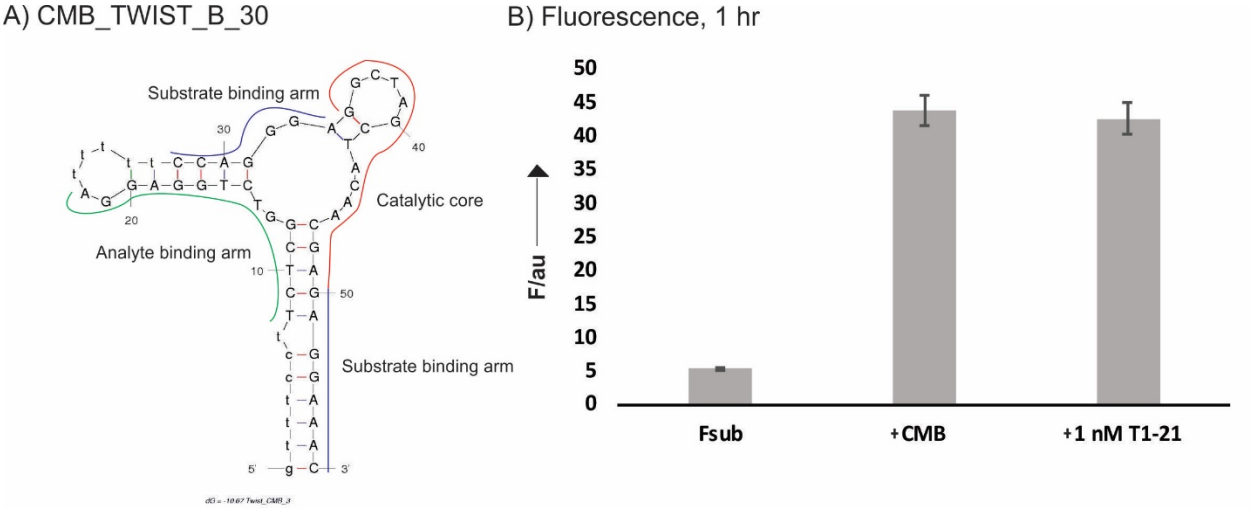

Figure 9. Structure and performance of CMB_TWIST_B_30. A) Mfold calculated structure that contains shorter binding arms and secondary structure to increase selectivity. Conditions for folding were 30ºC, 90 mM Mg2+, and 50 mM Na+. The structure was traced in green, blue and red to denote the analyte binding arm, substrate binding arm, and catalytic core, respectively. B) Fluorescent performance of sensor. F sub control contained 200 nM of F_sub in reaction buffer. '+CMB' control consisted of 200 nM F_sub and 5 nM CMB_TWIST_B_30. +1 nM T1-21 contained the same components as the +CMB control with the addition of 1 nM of T1-21 analyte. The samples were incubated at 30ºC for 1 hr and measured.

Table 2. Selectivity Factor (SF) and limit of detection (LOD) for each DZ probes used in this study

	Analytes	TºC	Assay time, hr	DF	LOD, pM
CMB	T1/T2	30	1	0.31	89.2
			3	UD[c]	80.7
	T1/T2	55	1	0.38	31
			3	UD	UD
	A1/A2	30	1	0.18	74.0
			3	UD	59.5
	A1/A2	55	1	0.07	UD[d]
			3	UD	UD[d]
BiDZ	T1/T2	30	1	0.83	164
			3	UD	26.2
	T1/T2	55	1	0.65	133
			3	UD	98
	A1/A2	30	1	0.84	47.1
			3	UD	15.3
	A1/A2	55	1	0.89	11.4
			3	UD	8.3

[a]SF was calculated by dividing the raw values of the matched analyte by the mismatched analyte for 5 nM analyte for the TWIST analyte and 1 nM for the AMELY analyte. Fluorescent intensities were measured after 1 hr of incubation. [b]LOD was determined by 3 individual trials after at 1 and 3 hrs or assay. [c]UD is undetermined. [d]UD due to high background signal. DF was calculated according to the formula: DF = 1-Fmm/Fm, where Fmm and Fm are average fluorescence of samples in the presence of T2(A2) and T1(A2) analytes respectively.

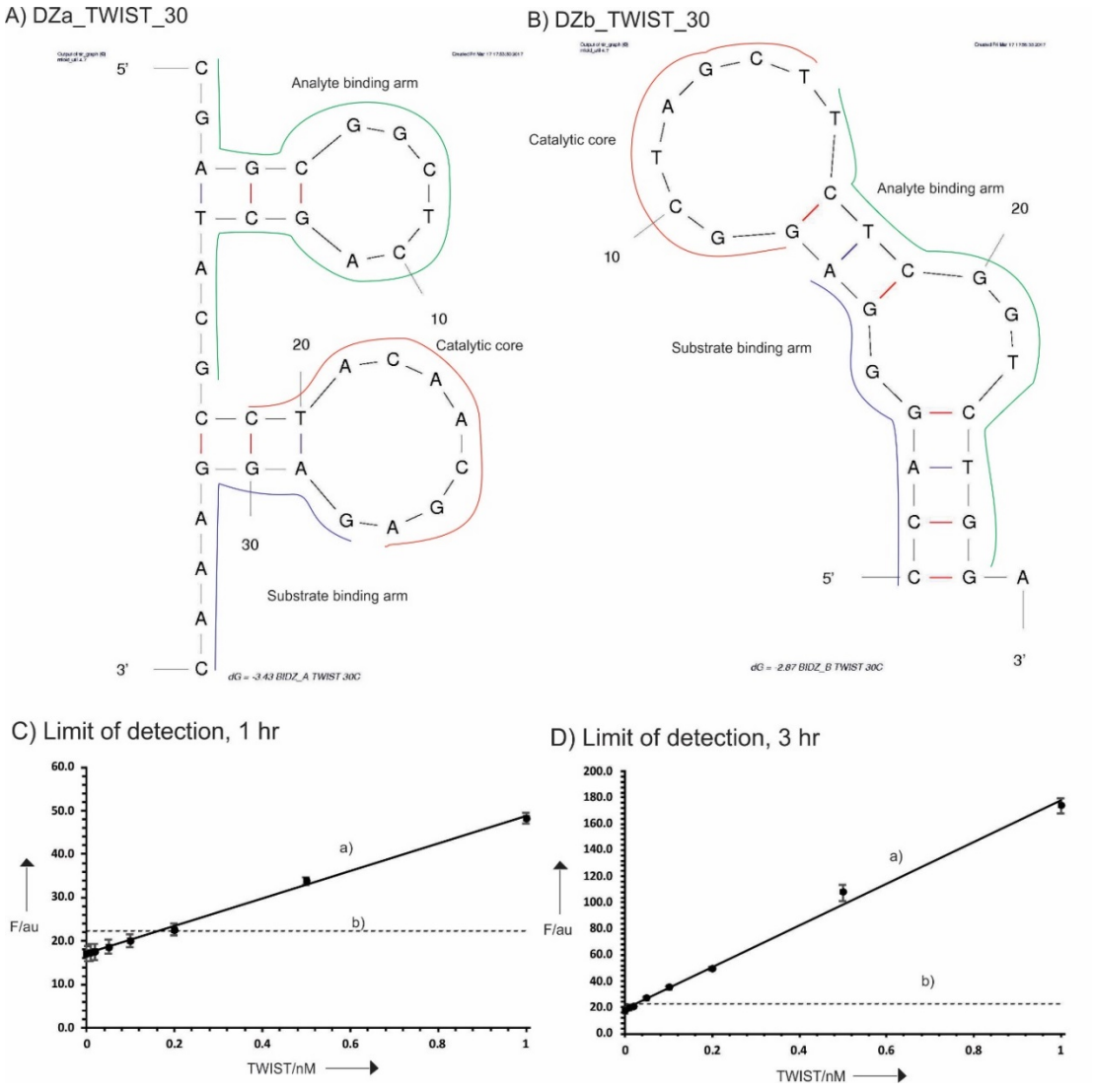

Figure 10**. BiDZ_TWIST_30** structure and performance. A) Mfold calculated structure for **Dza_TWST_30**. Conditions for folding were 30ºC, 90 mM Mg^{2+}, and 50 mM Na^{+}. B) Mfold structure for **Dzb_TWIST_30**. The structures were traced in green, blue and red to denote the analyte binding arm, substrate binding arm, and catalytic core, respectively. Samples contained 200 nM **F_sub**, 5 nM BiDZ, and various amounts of analyte (0 nM -0.2 nM) in reaction buffer. After 1 and 3 hrs incubation at 30ºC in a water bath the fluorescence was measured. C) Limit of detection for one hr hybridization was 164 pM (a) and the threshold (b) was calculated as three standard deviations above the control (0 nM analyte). D) Limit of detection after 3 hrs of reaction was 26.2 pM (a) and the threshold (b) was calculated as three standard deviations above the control (0 nM analyte).

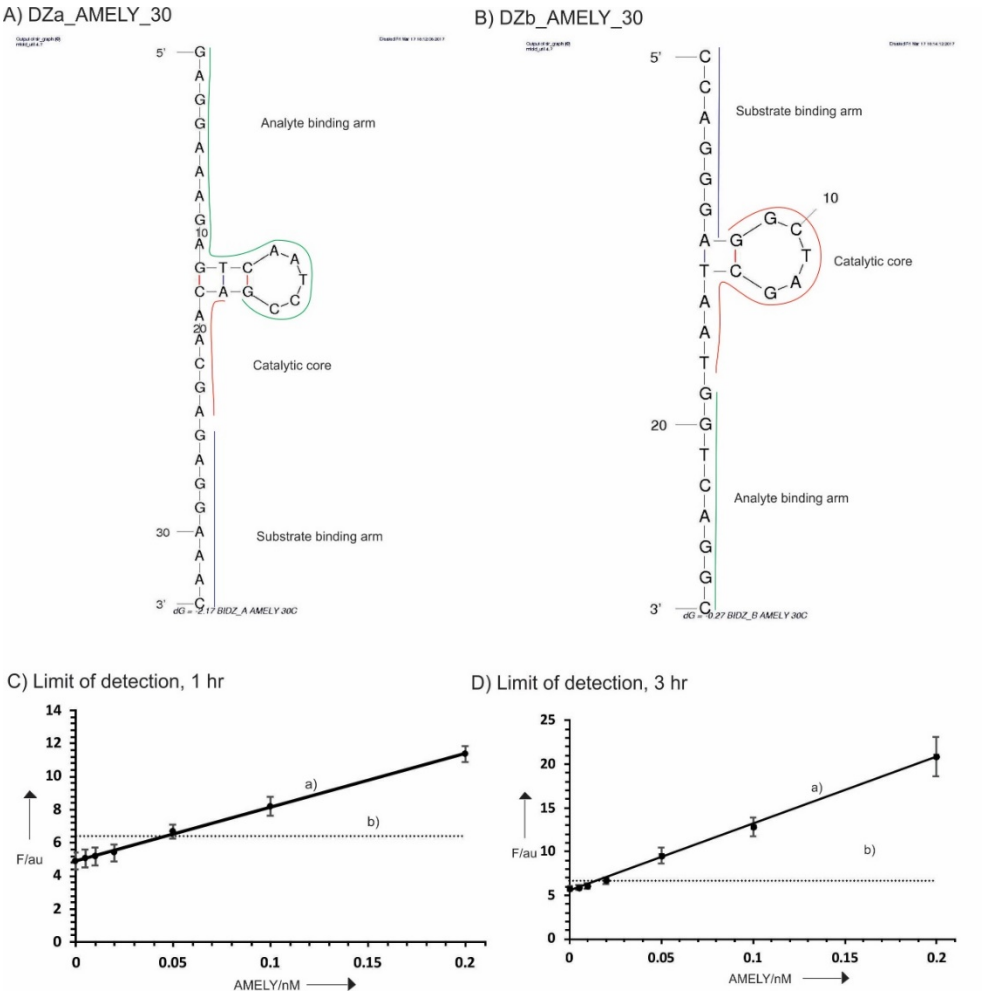

Figure 11. **BiDZ_AMELY_30** structure and performance. A) Mfold calculated structure for **Dza_AMELY_30**. Conditions for folding were 30ºC, 90 mM Mg^{2+}, and 50 mM Na^{+}. B) Mfold structure for **Dzb_AMELY_30**. Conditions for folding were 30ºC, 90 mM Mg^{2+}, and 50 mM Na^{+}. The structures were traced in green, blue and red to denote the analyte binding arm, substrate binding arm, and catalytic core, respectively. Samples contained 200 nM **F_sub**, 5 nM BiDZ, and various amounts of analyte (0 nM-0.2 nM) in reaction buffer. After 1 and 3 hrs incubation at 30ºC in a water bath the fluorescence was measured. C) Limit of detection for one hr hybridization was 47.14 pM (a) and the threshold (b) was calculated as three standard deviations above the control (0 nM analyte). D) Limit of detection for 3 hrs hybridization was 15.33 pM (a) and the threshold (b) was calculated as three standard deviations above the control (0 nM A1 analyte).

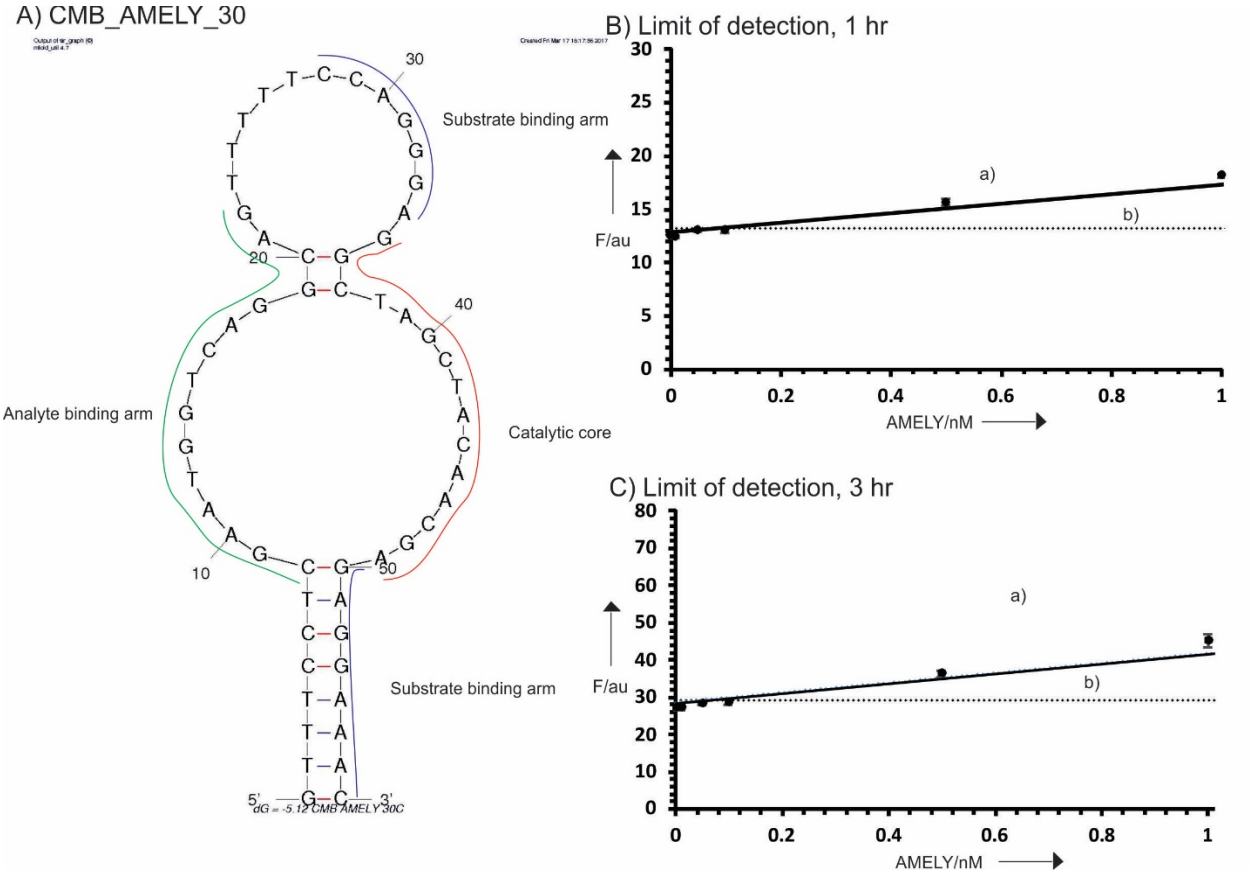

Figure 12. **CMB_AMELY_30** structure and performance. A) Mfold calculated structure. Conditions for folding were 30ºC, 90 mM Mg^{2+}, and 50 mM Na^{+}. The structure was traced in green, blue and red to denote the analyte binding arm, substrate binding arm, and catalytic core, respectively. Samples contained 200 nM **F_sub**, 5 nM CMB, and various amounts of analyte (0 nM -0.2 nM) in reaction buffer. After 1 and 3 hrs incubation at 30ºC in a water bath the fluorescence was measured. C) Limit of detection for one hr hybridization was 74 pM (a) and the threshold (b) was calculated as three standard deviations above the control (0 nM analyte). D) Limit of detection for 3 hrs hybridization was 59 pM (a) and the threshold (b) was calculated as three standard deviations above the control (0 nM A1 analyte).

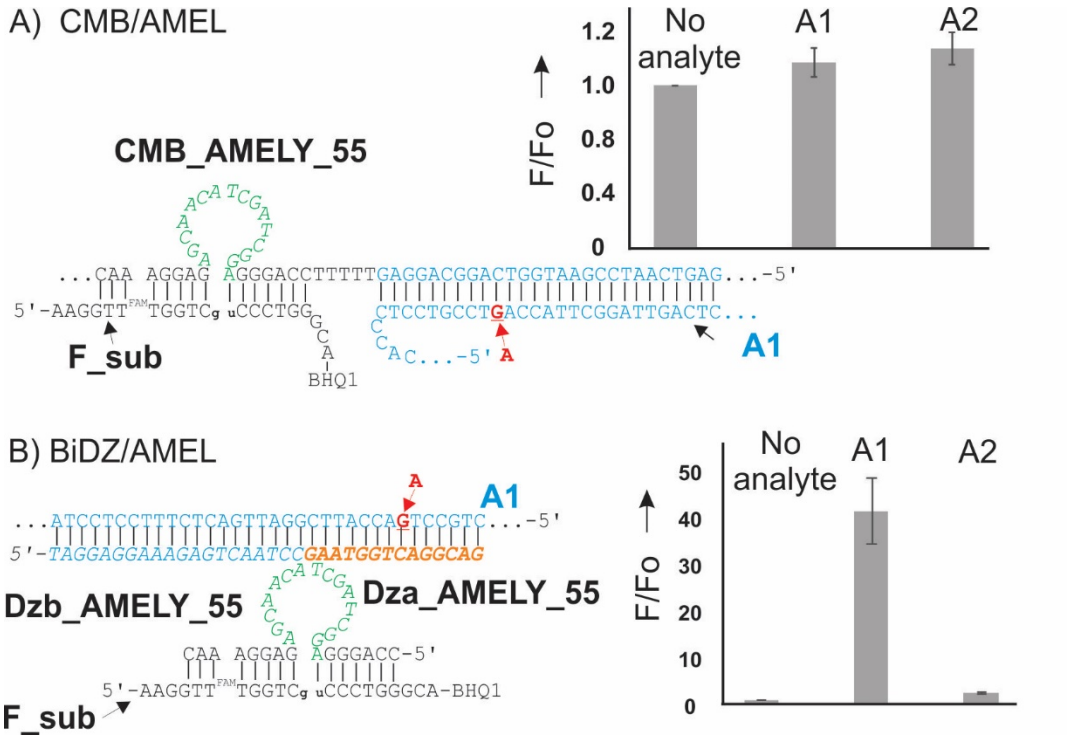

Figure 13. Predicted structures of probe-analyte complexes and selectivity data for CMB (A) and BiDz (B) recognizing **A1** analyte at 55ºC design. For right panels: all samples contained 200 nM **F_sub** and either 5 nM CMB or 5 nM DZa_T and 5 nM DZb_T in the reaction buffer. Samples A1 and A2 contained 1 nM complementary A1 and 1 nM mismatched A2 analyte, respectively (for full sequences see Table S1). Fluorescence intensity at 517 nm (emission at 485 nm) was measured after 1 hr of incubation. The data are average values of 3 independent experiments.

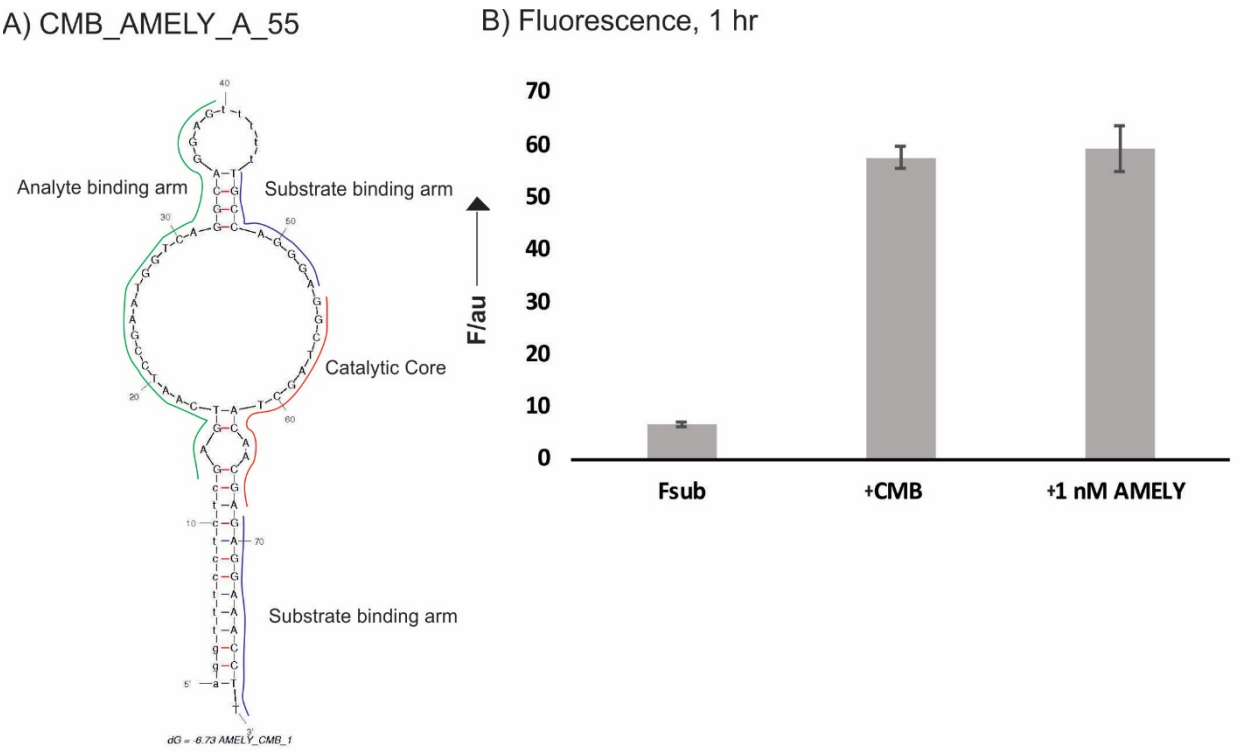

Figure 14. **CMB_AMELY_A_55** structure and performance with more stable stem for reduced leakage. A) Mfold calculated structure that contains a long stem to promote secondary structure to decrease sensor leakage. Conditions for folding were 55ºC, 50 mM Mg^{2+}, and 90 mM Na^{+}. The structure was traced in green, blue and red to denote the analyte binding arm, substrate binding arm, and catalytic core, respectively. B) Fluorescent performance of sensor. 'Fsub' control contained 200 nM of **F_sub** in reaction buffer. '+CMB control' contained 200 nM **F_sub** and 5 nM **CMB_TWIST_B_30.** Sample **'**+1 nM AMELY' analyte contained the same components as the '+CMB' control with the addition of 1 nM of **A1** analyte. The samples were incubated at 55ºC for 1 hr and measured.

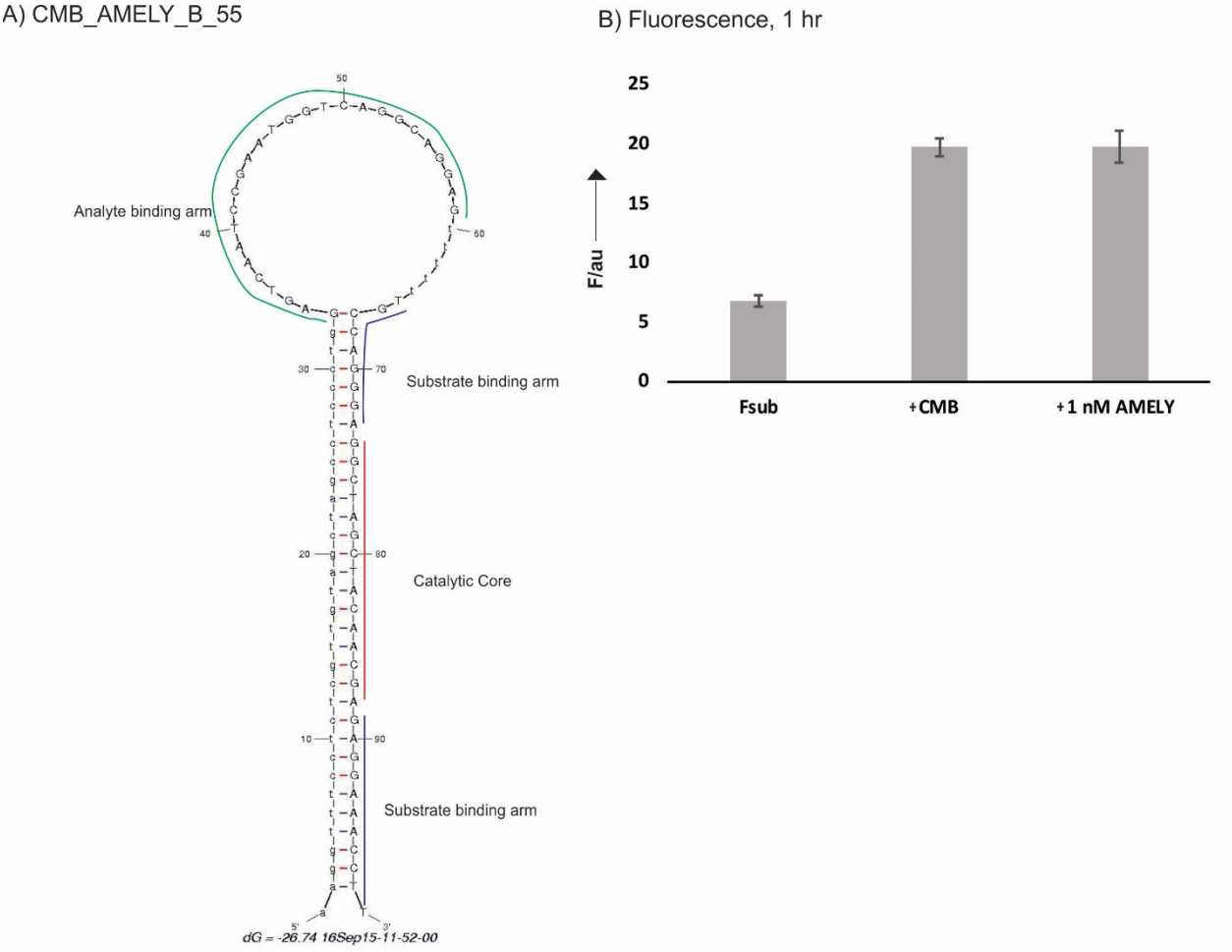

Figure 15. **CMB_AMELY_B_55** structure and performance for stability at higher temperatures. A) Mfold calculated structure that contains a 34 bp-long stem to promote stability at higher temperatures (55ºC). Conditions for folding were 55ºC, 90 mM Mg^{2+}, and 50 mM Na^{+}. The structure was traced in green, blue and red to denote the analyte binding arm, substrate binding arm, and catalytic core, respectively. B) Fluorescent performance of sensor. 'Fsub' control contained 200 nM of **F_sub** in reaction buffer. '+CMB control' consisted of 200 nM **F_sub** and 5 nM **CMB_AMELY_B_55**. Sample '+1 nM AMELY' contained the same components as the '+CMB' control with the addition of 1 nM of A1 analyte. The samples were incubated at 55ºC for 1 hr and measured.

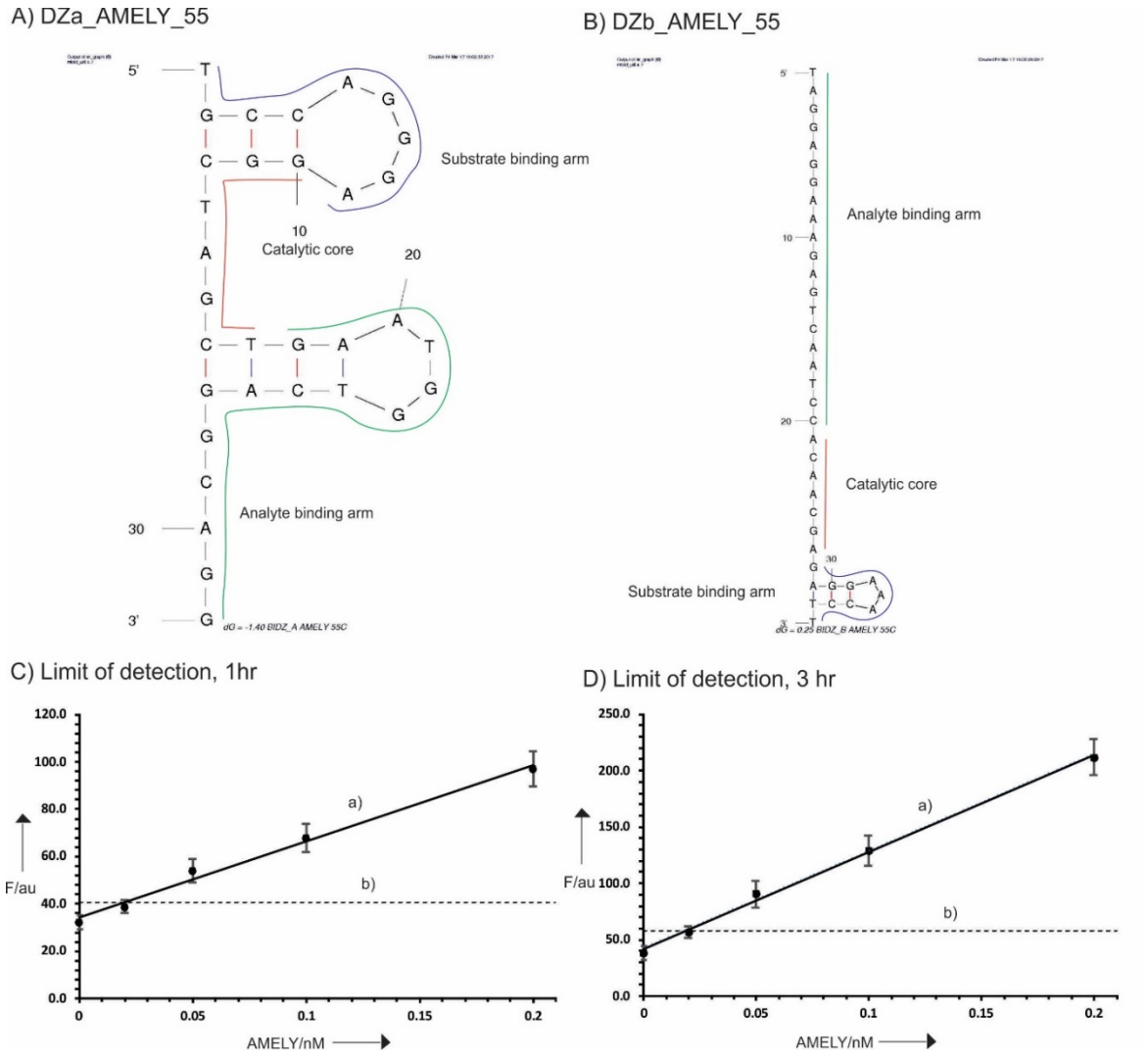

Figure 16**. BiDZ_AMELY_55** structure and performance. A) Mfold calculated structure for **Dza_AMELY_55**. Conditions for folding were 55ºC, 90 mM Mg^{2+}, and 50 mM Na^{+}. B) Mfold structure for **Dzb_AMELY_55**. Conditions for folding were 55ºC, 90 mM Mg^{2+}, and 50 mM Na^{+}. The structures were traced in green, blue and red to denote the analyte binding arm, substrate binding arm, and catalytic core, respectively. Samples contained 200 nM **F_sub**, 5 nM BiDZ, and various amounts of analyte (0 nM -0.2 nM) in reaction buffer. The fluorescence was measured after 1 and 3 hrs incubation at 55ºC. C) Limit of detection for one hr hybridization was 11. 4 pM (a) and the threshold (b) was calculated as three standard deviations above the control (0 nM analyte). D) Limit of detection after 3 hrs of reaction was 8.3 pM (a) and the threshold (b) was calculated as three standard deviations above the control (0 nM analyte).

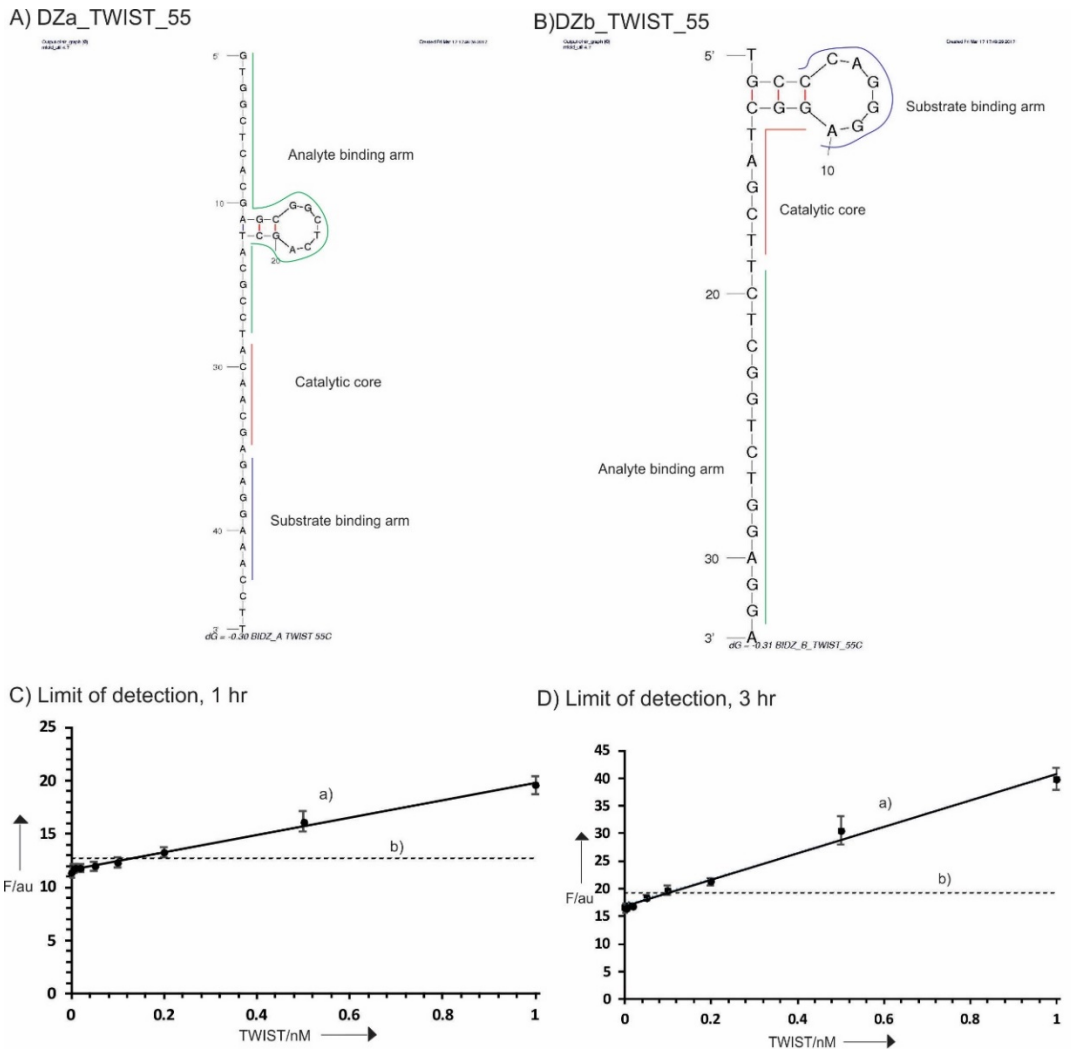

Figure 17. **BiDZ_TWIST_55** structure and performance. A) Mfold calculated structure for **Dza_TWIST_55**. Conditions for folding were 55ºC, 90 mM Mg^{2+}, and 50 mM Na^{+}. B) Mfold structure for **Dzb_TWIST_55**. Conditions for folding were 55ºC, 90 mM Mg^{2+}, and 50 mM Na^{+}. The structures were traced in green, blue and red to denote the analyte binding arm, substrate binding arm, and catalytic core, respectively. Samples contained 200 nM **F_sub**, 5 nM CMB, and various amounts of analyte (0 nM -0.2 nM) in reaction buffer. After 1 and 3 hrs incubation at 55ºC in a water bath the fluorescence was measured. C) Limit of detection for one hr hybridization was 133 pM (a) and the threshold (b) was calculated as three standard deviations above the control (0 nM analyte). D) Limit of detection for 3 hrs hybridization was 98 pM (a) and the threshold (b) was calculated as three standard deviations above the control (0 nM analyte).

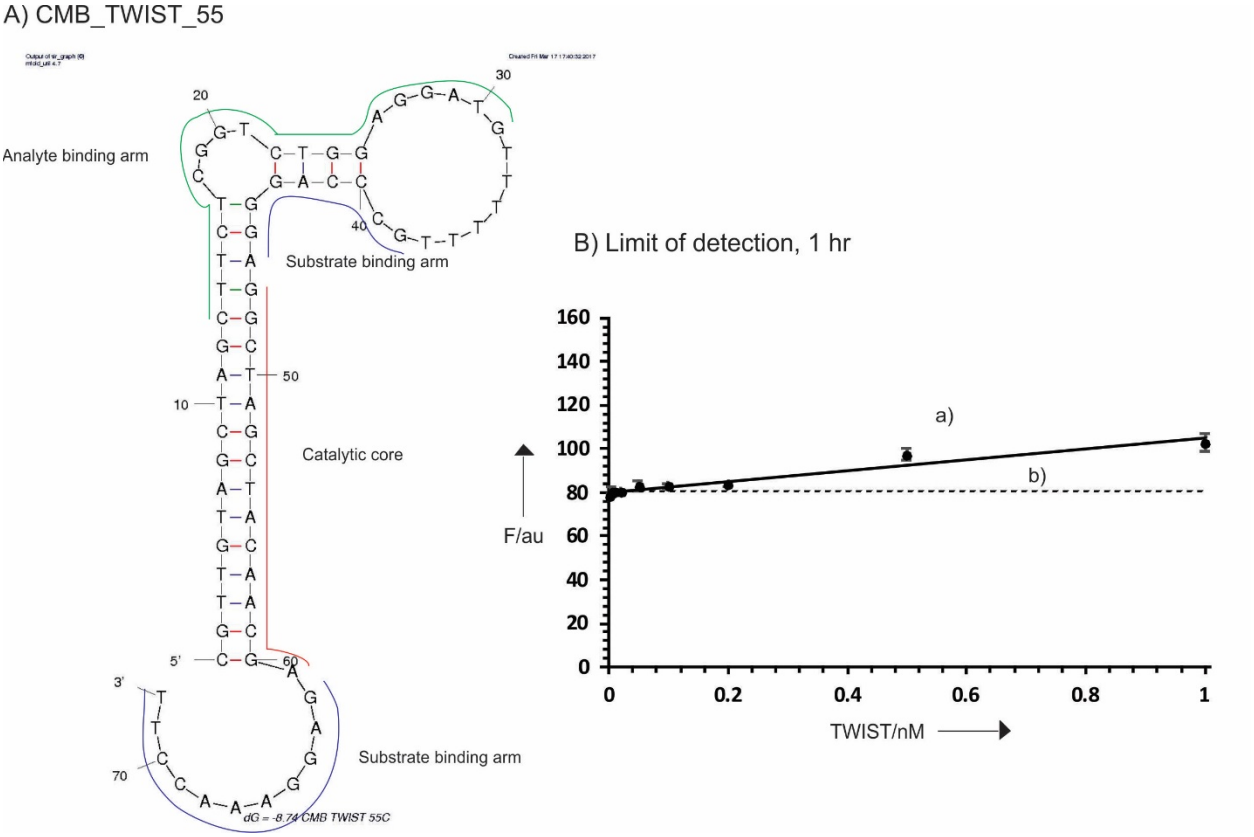

Figure 18**. CMB_TWIST_55** structure and performance. A) Mfold calculated structure. Conditions for folding were 55ºC, 90 mM Mg^{2+}, and 50 mM Na^{+}. The structure was traced in green, blue and red to denote the analyte binding arm, substrate binding arm, and catalytic core, respectively. Samples contained 200 nM **F_sub**, 5 nM CMB, and various amounts of analyte (0 nM -0.2 nM) in reaction buffer. After 1 and 3 hrs incubation at 55ºC in a water bath the fluorescence was measured. C) Limit of detection for one hr hybridization was 31 pM (a) and the threshold (b) was calculated as three standard deviations above the control (0 nM analyte). A three hr time point for limit of detection was inconclusive with a R^2 value of 0.8423.

CHAPTER THREE: SEX DETERMINATION OF MODERN HUMAN REMAINS

Sex identification of unknown remains is crucial to personal identification of human remains in anthropology and forensics. When conventional methods, such as metric or morphological analyses, are not an option due to the fragmented or prepubescent remains, molecular diagnostics are needed. The amelogenin gene, found on sex (X and Y) chromosomes, is the most common molecular marker used for sex determination because it exhibits sexual dimorphism in size and sequence. Here we develop a new method for fluorescent analysis of amelogenin gene for sex identification. In this assay, human DNA is amplified during a period of 30 min by isothermal loop mediated amplification (LAMP) followed by analysis by a binary deoxyribozyme sensors for 60 min. High selectivity of the amelogenin sequences of Y and X chromosome was demonstrated. The assay requires a hot plate and a portable fluorimeter and thus can be used at point of excavation or a crime scene at a remote location for forensic laboratories. The assay promises to simplify molecular-based sex determination of human remains.

Introduction

Identifying the sex of human remains is an important part of the biological profile. When intact skeletons are present sex determination can be done by conventional methods, but when only fragments or the skeleton is a juvenile are obtainable the determination of sex is difficult. Studies have been done on the pelvis[12] and cranium[17] where the bones were measured to determine sex. Metric analysis obtains 98% to 100% accuracy in sex estimation. The overall

obstacle lies within partial adult skeletal remains, or juvenile remains, in which only 70% accuracy is obtained using metric analyses.

The Amelogenin gene, found on both sex chromosomes, is the most widely used target for molecular sexing. Originally sequenced by Nakahori et al[33], the gene contains sequence and size divergences between the X and Y chromosomes making it the perfect target for our proposed platform. The Amelogenin gene codes for the production of tooth enamel and is a highly conserved sequence found on each sex chromosome. AMELX-allele has a size of 2872 bp and is located on the Xp22.1-Xp22.3 region of the X-chromosome, while AMELY-allele has a size of 3272 bp is located on the Yp11.2 region of the Y chromosome[32]. Also, there is a 3-bp deletion on the AMELX-allele compared to the AMELY-allele in a certain region allowing for dimorphism.

PCR is the conventional amplification method used for molecular-based diagnostics. A method proposed by Alvarez-Sandoval et al. uses real-time PCR amplification followed by High Resolution Melting analysis (HRM)[34]. Another HRM analysis used SYBR Green as a DNA binding dye and differential melting curves[35]. Unfortunately, this dye has the ability to inhibit PCR, promote mispriming, and lacks stability overtime. It also has been known to produce unreliable melting curves due to the "dye redistribution" phenomenon[36]. Isothermal loop mediated amplification is a simple amplification method. Unlike PCR, no thermal cycler is needed. Typical amplification takes 60 min but can be achieved as short as in 15 min. LAMP requires 5-7 primers and amplifies the target sequences into various size fragments. Designing the multiple primers can be tedious, but DNA at the concentration up to 1 μM can be produced;

which is about an order of magnitude higher than that of a typical PCR amplicon[38b]. LAMP products for sex identification have been previously achieved using a visual method[58]. As the DNA is being amplified the solution will become turbid, visually allowing for conformation of the target sequence. Similar LAMP primers were used in our experiment. However, we used fluorescent readout produced by a deoxyribozyme sensor, which ensured high selectivity of target recognition..

Deoxyribozymes, or DNA enzymes, are catalytic deoxyribonucleotides derived by *in-vitro* selection[1,2] . Catalytic DNA offers high chemical stability, low cost for synthesis, biocompatibility, and ease of structural prediction and modification[5]. Binary deoxyribozyme have shown to be a useful platform for nucleic acid detection due in part to their improved sensitivity, which is achievable by catalytic amplification of the positive signal. Binary probes are more selective than conventional proves because each relatively short hybrid (7-10 nucleotides for the target binding region) is extremely sensitive to single-base mispairings. There have been several applications for deoxyribozyme sensors including ion detection [7], and breast cancer treatment[9]. The binary deoxyribozyme sensor proposed herein is comprised of two probes: DZa and DZb (**Figure 19A**). Each probe contains a substrate binding arm and an analyte binding arm. A reporter, the F sub (**Figure 19A**), contains a fluorophore and quencher conjugated to the opposite ends of the oligomer. When the F substrate binds to both probes it can be subjected to cleavage upon binding of the analyte allowing for a fluorescent signal to be detected. The specificity of nucleic acid recognition is increased by the two components of the probe. Combining a binary deoxyribozyme sensor with a rapid and isothermal amplification technique aims to simplify the field of molecular –based human sex determination.

Materials and Methods

DNAse/RNAse free water was purchased from Fisher Scientific, Inc. (Pittsburgh, PA, USA) and used for all buffers and for the stock solutions of oligonucleotides. Oligonucleotides were custom made by Integrated DNA Technologies, Inc. (Coralville, IA, USA) and by TriLink BioTechnologies, Inc. (San Diego, CA, USA) with standard desalting (SD). Fluorescent spectra was measured with a Perkin-Elmer (San Jose, CA, USA) LS-55 luminescence spectrometer with a Hamamatsu xenon lamp at excitation 485 nm and emission 517 nm; data were processed by using Microsoft Excel.

Detection of synthetic analyte

F_sub (200 nM) and sensor strands, Dza/Dzb, (5 nM) for X sensor and Y sensor were incubated with various concentrations of analytes in the reaction buffer (50 mM HEPES, pH7.4, 50 mM MgCl2, 20 mM KCL, 120 mM NaCl, 0.03% Triton X-100, 1% DMSO). After 1 or 3 hour of incubation at 55^{o}C, the fluorescence of the samples was measured at 517 nM at room temperature. Control samples contained only F sub and sensor strands. The average values of three independent experiments were plotted as a function of analyte concentration.

Selectivity Experiments

F_sub (200 nM) and sensor strands, Dza/Dzb, (5 nM) for X sensor and Y sensor were incubated in the presence of either the matched analyte or mismatched analyte (1 nM). The control sample did not contain any analyte and consisted of only **F_sub** (200 nM) and sensor strands, Dza/Dzb, (5 nM). After 1 hr of incubation at 55^{o}C the sample fluorescence was measured at 517 nM (λ_{ex} = 485 nm) at room temperature. 3 independent experiments were run.

DNA extraction

The sample was first decontaminated by grinding away 2 mm from the surface of the sample using a Dremel tool (Racine, WI) to remove contaminating DNA. The tooth was then immersed in a 20% (v/v) bleach solution and sonicated for ~6 min. Following a wash with UV-irradiated DI water, the sample was sonicated for an additional 5 minutes. Then the sample was rinsed in 95% ethanol and placed in a sterilized fume hood to dry overnight. After decontamination, the outer surface of part of the specimen was removed with a Dremel tool. A piece of the dentin or the root was isolated and grinded with mortar and pestle until a fine-grained powder was obtained. Qiagen investigator kit was used to purify the DNA; the protocol from the manufacturer was followed. DNA was quantified using UV-Vis (Perkin Elmer, Lambda 35) and stored at room temperature, in the dark. All LAMP components, excluding primers, were obtained from New England Bio Labs (Ipswich, MA).

LAMP amplification

Each sample contained 1x isothermal buffer, 1.4 mM dNTPs, 6 mM $MgSO_4$, 2.0 µM FIP/BIP primers, 0.2 µM F_3/B_3 primers, 0.8 µM Loop primer, 0.16 pg/µL to 0.160 pg/µL template, and 1 µL/25 µL reaction for Bst enzyme. The reaction was mixed in an Eppendorf tube and heated in a water bath at 65^{o}C for 15-60 minutes. The samples were then placed on ice or in a -20^{o}C freezer. The primers were either X- or Y-specific were designed following H. Nogami et al (2008). The reaction was analyzed using gel electrophoresis to ensure amplification. For the varying amplification times, all samples were mixed at the same time and incubated together at 65^{o}C. Once the time point was reach, the sample tube, for the respective time point, was removed from the water bath.

Detection of LAMP amplified DNA

F_sub (200 nM) and sensor strands (DZA/DZB) (5 nM) were incubated with 5-20 µL of LAMP amplified DNA in 1x reaction buffer (100 mM HEPES,pH7.4, 100 mM $MgCl_2$, 40 mM KCL, 240 mM NaCl, 0.06% Triton X-100, 2% DMSO) and diluted with water to a final volume of 60 µL. Control samples consisted of F substrate, F substrate and probe strands , 1 nM of synthetic AMEL analyte, and LAMP product with no template. After 1 hour of incubation at 55^{o}C, fluorescence was measured at 517 nM (excitation at 485 nM).

Results and Discussion

First we characterized DZ sensors using synthetic DNA analytes with the targeted sequences AMELX and AMELY. It was found that detection limits for the X sensor and for Y sensor were determined to be 38 pM (**Figure 20**) and 11 pM (**Figure 21**), respectively. The sequences of the target analytes and their corresponding sensors are shown in **Table 4**. Further characterization involved examining the selectivity of each sensor. The X sensor showed no affinity for the AMELY analyte, with no signal above the background and s/b ratio of 3 for AMELX (**Figure 19B**). Similar results were shown for the Y sensor, a high s/b of 10 for the AMELY analyte and no detection of the AMELX analyte (**Figure 19C**).

Using LAMP amplification, sex determination of teeth samples was achieved by the BiDZ sensors. DNA was extracted from one adult female tooth and one juvenile male tooth. The female tooth had been stored at room temperature for 3 years and the juvenile tooth was stored at room temperature for approximately 14 years. 20 µl of the LAMP products were targeted by X sensor and Y sensors after amplification with the X- or Y-specific primers. Amplification

occurred with 0.16 ng/µl template that was amplified for 15 to 60 minutes, and amplification was confirmed by gel electrophoresis (**Figure 22**). The background (NC) consisted of all the LAMP components and no DNA templated. Several different size bands are shown because the target sequence is amplified several times in various length fragments. This is due to the looping mechanism of LAMP, in which a dumbbell shape fragment is created and continues amplification after each loop. 30 minute amplification was chosen because an ample amount of DNA was produced and the NC showed little contamination. **Figure 23A** shows the successful amplification with X primers and Y primers for female DNA for 30 minutes. The bands for the XX sample were darker than NC (no template) for X primers proposing more amplified DNA was present in the XX sample. The NC and XX amplified by Y primers look to be of similar intensities. The difference in the X primer samples was reflected in the fluorescent assay (**Figure 23B**) with XX having a higher signal than NC for the X sensor. The selectivity of the BiDZ sensor is shown with the Y sensor, which produces a signal below the background for female DNA even with contamination present. This quenching affect can be attributed to the sensor probes hybridizing, separately, to non-specific DNA and disrupting the catalytic core.

Male DNA was successfully amplified by X primers and Y primers (**Figure 23C**). For the samples amplified with X primers, NC contains darker bands than XY, which led us to believe the concentration of amplicon was higher in the NC sample, but this is not reflected by the BiDZ results (**Figure 23D**). For the X sensor the target sequence in the XY sample was present at higher concentrations as seen by the fluorescent signal above NC. NC (Y primers) contained no contamination and produced a low signal. XY (Y primers) was successfully amplified and detected above the background for the Y sensor.

Ultimately the Y sensor allows for differentiation between male and female. With s/b ratio of 1.5 deemed as the threshold, a parameter for sex determination using the Y sensor was developed (**Table 5**). The 50% increase in signal equates to the 3σ (99%) confidence interval, based on a typical standard deviation σ ~ 15% of the measured fluorescent signal[59]. The X sensor can serve as a control test for the presence of human DNA. If the output signal is 1.5 higher than the background, the sample considered reliable. Samples 1-3 are separate female LAMP samples, originating from the same tooth source, and produced s/b ratio greater than 1.5 for the X sensor. For the Y sensor no s/b ratio above 1 was produced, confirming the correct genetic sex of the female adult tooth. Samples 4-7 are separate male LAMP samples, originating from a single juvenile tooth. 4 out of 4 male LAMP samples detected by the X sensor had s/b ratio above 1.5. For the Y sensor only 3 out of the 4 samples had s/b ratios above 1.5. Sample 7's genetic sex did not match the known morphological sex. This could be due to the non-specific amplification, lowering the amount of the target sequence, thus rendering a low fluorescent output signal. Since LAMP incorporates 5 primers, there are several sites were amplification can occur. Y-specific amplification can be optimized by redesigning the primer set to a more unique region of the gene sequence to increase the amount of the target sequence and decrease non-specific amplification.

With a total time of one hour and forty five minutes (15 minutes sample prep, 30 minutes amplification, 1 hour sensing), we have developed an attractive method for sex determination. Heating can be done on a hot plate with water for amplification at 65ºC and sensing at 55ºC. Fluorescent detection can be done using a portable fluorimeter allowing for sex determination on site for anthropological purposes or at crime scene.

Figures and Tables

Table 3. LAMP primers

Name	Sequence 5'→3'
AMELX FIP	AGC ACG GGG ATG ATT TGG TGC CCT TCC TAT GGT TAC GAG
AMELX BIP	CCT CAT CAC CAC ATC CCA GTG CAG GAA CGG GCA TCA TTG
AMELX B3	GGA TTG GAG TCA TGG AGT G
AMELX F3	TGC CTC TCT CTT TCT CAC
AMELX Loop R	TGC AGC CAT CCA CCC AT
AMELY FIP	AAT CCG AAT GGT CAG GCA GGC CAG TTT AAG CTC TGA TGG TT
AMELY BIP	GAC TCT TTC CTC CTA AAT ATG GCT GTT TTG CCC TTT CAT GGA AC
AMELY B3	CTG GTC AGT CAG AGT TGA C
AMELY F3	GGT CCC AAT TTT ACA GTT CC
AMELY Loop F	GGT GCT GGA GCA ACA CAG

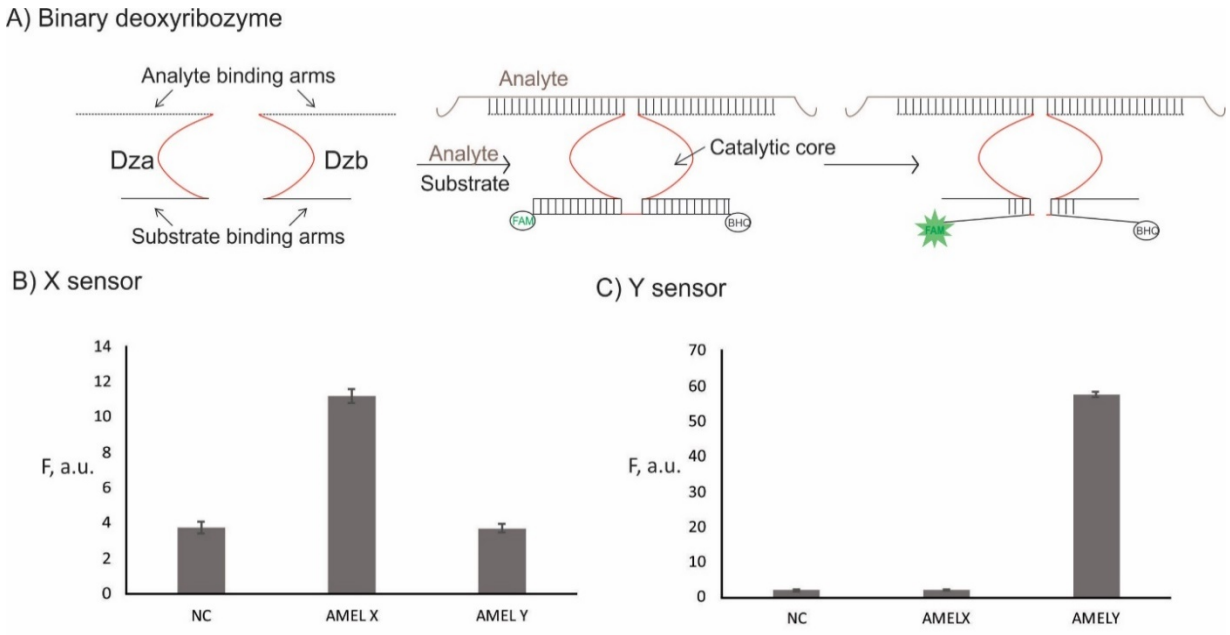

Figure 19. X and Y sensor performance. A) Schematic of a binary deoxyribozyme sensor containing two probes, Dza and Dzb. Upon addition of the analyte the catalytic core (red) will form and cleave the substrate. B) X sensor with NC (no analyte), AMELX analyte (1 nM) and AMELY (1 nM) to show the selectivity of the sensor. C) Y sensor with NC (no analyte), AMELX (1 nM), and AMELY (1 nM). Both assays contained 5 nM of Dza and Dzb with 200 nM of F_sub and were incubated for 1 hour at 55^{o}C.

Table 4. Sequences for chromosome-specific analytes and BiDZ probes

Name	Sequence 5→3
AMEL_X	GGC TGC AGG GTG TGA GTC GG GGGG TGC TGT TGG GAC AGC
AMEL_X DZ-A	TGC CCA GGG A GGCTAGCT CCC GAC TCA CAC CCT GCA GCC
AMEL_X DZ-B	GCT GTC CCA ACA GCA CCC A CAA CGA GAGGAAACCTT
AMEL_Y	CTC CAG CAC CCT CCT GCC TGA CCA TTC GGA TTG ACT CTT TCC TCC TAA ATA TGG CTG TAA GTT TAT TCA T
AMEL_Y DZ-A	TGC CCA GGG AGG CTA GCT ATC CGA ATG GTC AGG CAG GAG
AMEL_Y DZ-B	CCA TAT TTA GGA GGA AAG AGT CAA CAA CGA GAG GAA ACC TT

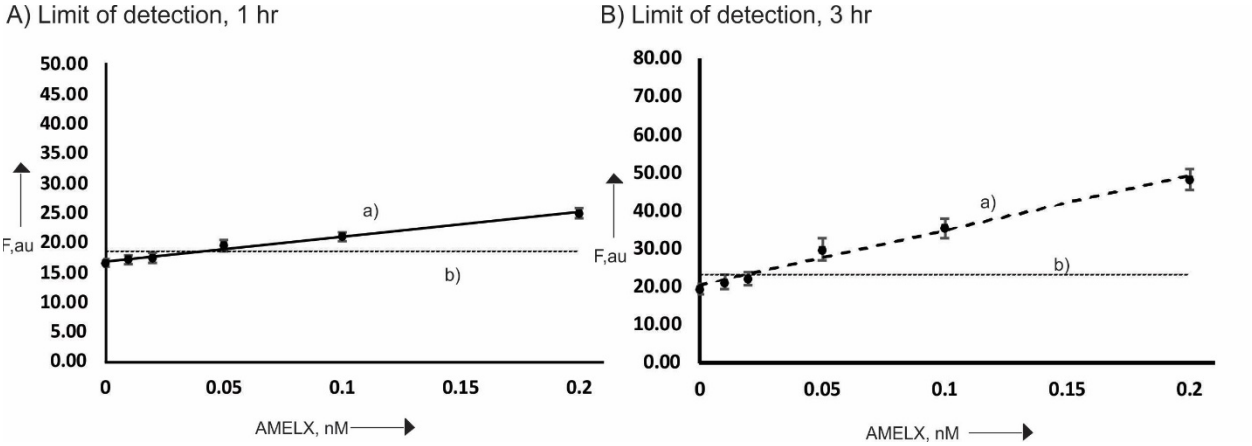

Figure 20. Limit of detection for the X sensor. 200 nM **F_sub**, 5 nM BiDZ X probes, and reaction buffer were mixed with varying concentrations of synthetic analyte (0-0.2 nM) and incubated at 55ºC. After 1 hr (A) and 3 hr (B) time points, the fluorescence was measured at an excitation of 517 nm. The linear trendline is denoted by a) and the threshold, calculated by 3 standard deviations above the negative control (0 nM analyte) is denoted by b).

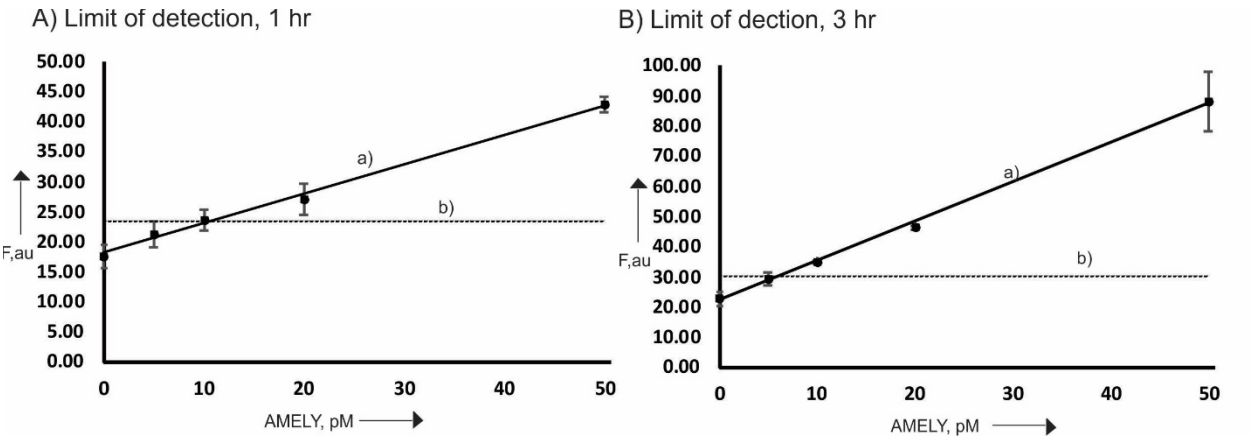

Figure 21. Limit of detection for the X sensor. 200 nM **F_sub**, 5 nM BiDZ X probes, and reaction buffer were mixed with varying concentrations of synthetic analyte (0-0.2 nM) and incubated at 55ºC. After 1 hr (A) and 3 hr (B) time points, the fluorescence was measured at an excitation of 517 nm. The linear trendline is denoted by a) and the threshold, calculated by 3 standard deviations above the negative control (0 nM analyte) is denoted by b).

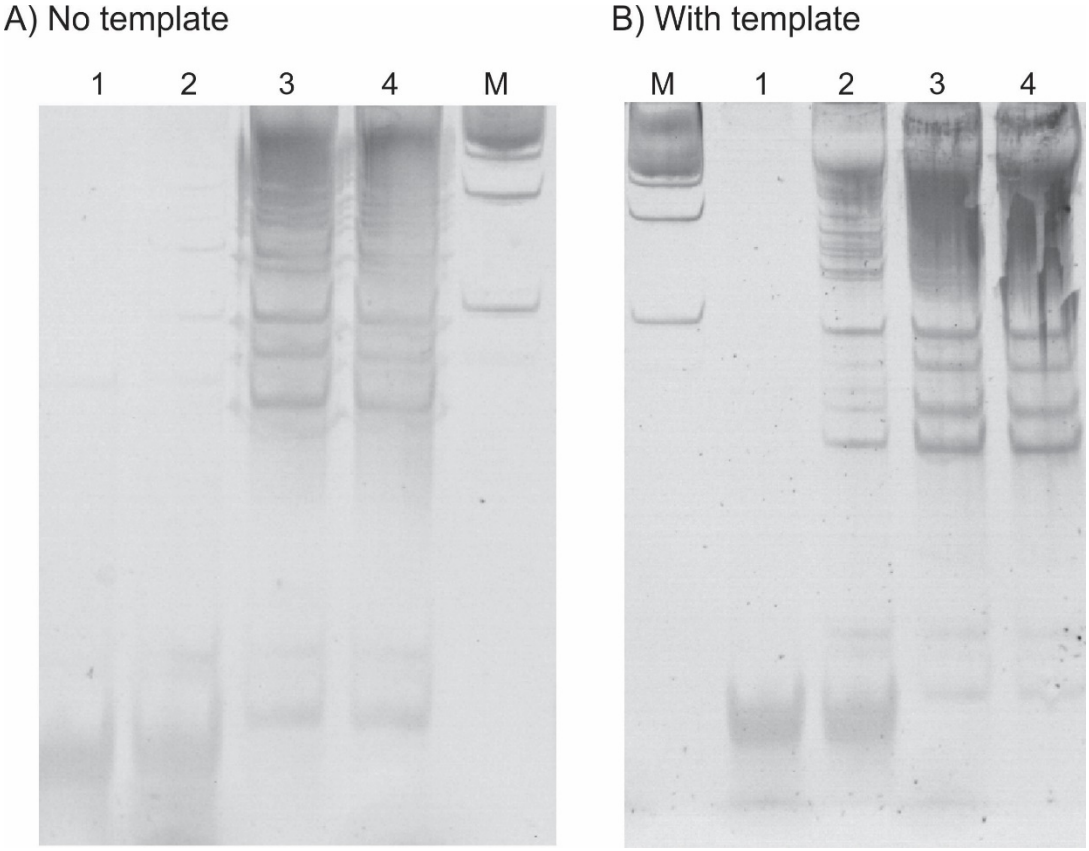

Figure 22. Amplification time optimization. A) No template was added to the amplification mixture and B) 2 ng of female DNA was added. X-specific primers were used for both images. Lane 1- 0 min, lane 2-15 min, lane 3- 30 min, lane 4- 60 min, and M contained 100 base pair ladder.

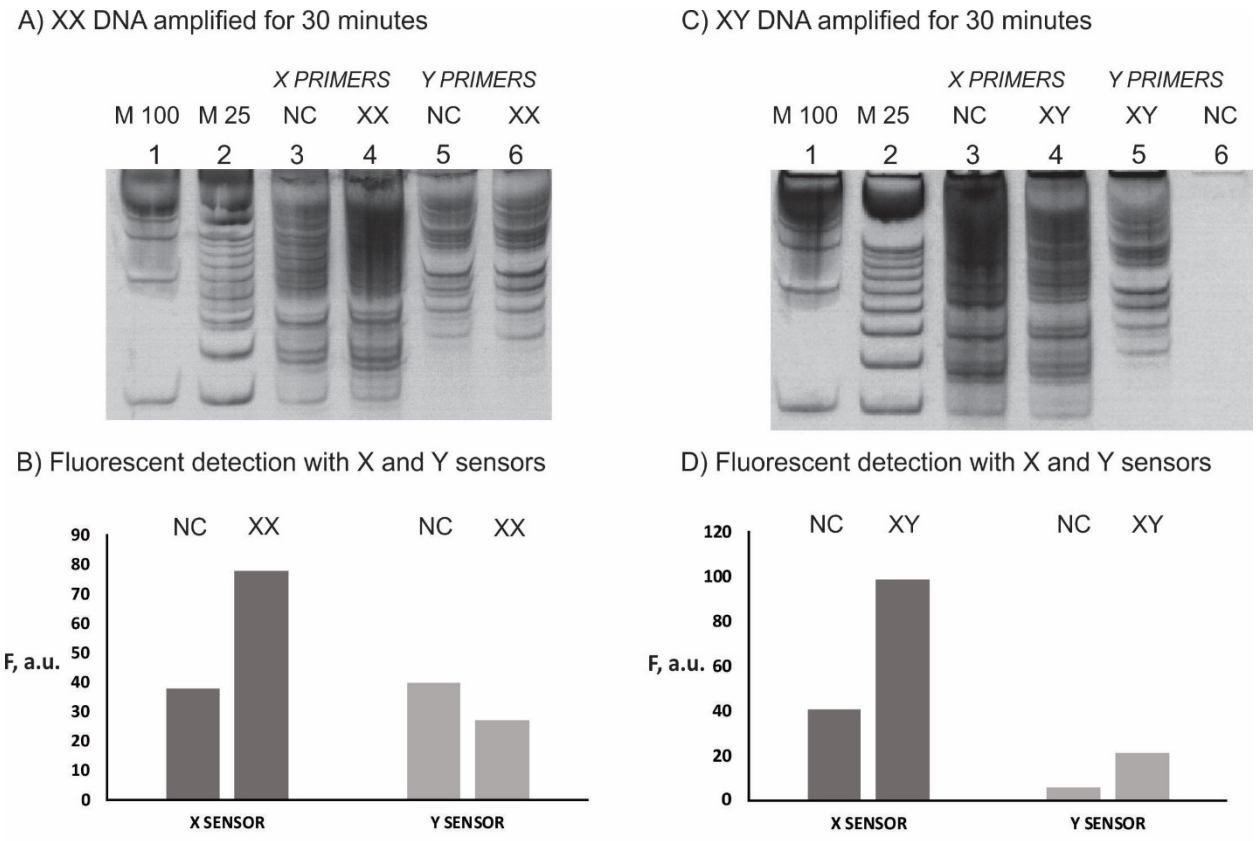

Figure 23. Sex determination of female and male teeth. Gel electrophoresis images show amplification for 30 minutes for A) Female DNA and C) Male DNA. A) contains Lane 1, 100 bps ladder; Lane 2, 25 bps ladder; Lane 3, negative control (0 DNA added) amplified by X primers; Lane 4, XX DNA (0.16 pg/µL) amplified by X primers; Lane 5, negative control (no DNA added) amplified by Y primers; Lane 6, XX DNA (0.16 pg/µL) amplified by Y primers. C) Lanes 1-4 correspond to A); Lane 5, XY DNA amplified by Y primers; Lane 6 negative control (no template added) amplified by Y primers. B) Female samples and D) male samples were incubated for 1 hour at 55^{o}C and detected with the both X and Y sensors. Samples amplified with X primers was detected by the X sensor. Samples amplified by Y primers were detected by the Y sensor. 200 nM F_sub, 5 nM BiDz, reaction buffer, and 20 µL of sample were used for detection.

Table 5. Sex determination results of teeth from known sex

Tooth Batch Number*	Morphological Sex	BiDz Results**		Genetic Sex***
		X sensor	Y sensor	
1	Female	1.6	0.82	Female
2	Female	2.43	0.88	Female
3	Female	3.0	0.87	Female
4	Male	2.43	2.91	Male
5	Male	4.20	1.95	Male
6	Male	3.02	1.61	Male
7	Male	1.85	0.87	Female

*Batches 1, 2, 3 originated from 1 adult female tooth, but were amplified separately.
*Batches 4, 5, 6, 7 originated from 1 juvenile male tooth, but were amplified separately.
**Calculated using the equation F_{+DNA}/F_{-DNA}.
***Genetic sex was determined has female with a result less than 1.5 and male with a result greater than 1.5 for the Y sensor. S/B ratio of 1.5 has been proven to show statistical difference with fluorescent measurements.

CHAPTER FOUR: CONCLUSIONS

Stemming from the discovery of ribozymes, deoxyribozymes became of interest due to the structural similarity between RNA and DNA. If RNA contains the ability to catalyze cleavage of nucleotides, than DNA could potentially possess the same ability. RNA and DNA only differ by a ribose 2'-hydroxyl group, yet there are no naturally occurring deoxyribozymes known. Particular DNA sequences have been found, by in vitro methods, to possess the ability to act as catalyst. There are multiple deoxyribozymes that cleave different targets and function under different conditions. For instance, some sensors rely on the presence of Pb^{2+} to be active, while others need Mg^{2+}. Deoxyribozyme sensors are now very promising artificial instantaneous hybridization probes. They can be used for fluorescent detection and compete with other platforms, such as real time PCR and molecular beacons, in the area of molecular diagnostics. Molecular diagnostics use DNA or RNA hybridization to detect a desired sequence and can be used to identify a vast range of targets. If the target sequence is known, the molecular probe simply has to be adjusted for that specific target. Real time PCR uses a taqman probe that contains a fluorophore and quencher on opposing sides of a short nucleotide sequence. The probe hybridizes to the target that is being amplified. As the target is produced, the DNA polymerase digest the probe, separating the quencher from the fluorophore, and producing a signal. A molecular beacon is a generic hairpin, which contains a fluorophore and quencher that are in close proximity because of the stem of the hairpin. Inside the stem loop, is the complementary sequence to the target. When the target is present it opens up the stem loop, and thus the fluorophore is now farther away from the quencher. Currently, using a deoxyribozyme in a form similar to that of a molecular beacon is most popular.

The advantage of deoxyribozymes over conventional molecular beacons is catalytic enhancement of signal, detection of dsDNA, and single base substitution differentiation. A molecular beacon can only bind one target and produce one signal, whereas the deoxyribozyme sensor can repeatedly cleave multiple substrate molecules by binding only one target. In this form the sensor undergoes a conformational change upon binding the analyte, which allows for the catalytic core to be able to bind the fluorogenic substrate. A typical catalytic molecular beacon possess lower limits of detection compared to conventional molecular beacons (pM vs. nM), but both cannot distinguish between a single nucleotide substitution. We have investigated the deoxyribozyme as a self-assembly driven sensor compared to its conformational 'switch' mechanism. The deoxyribozyme was split into two probes each containing part of the sequence that contains catalytic activity and further elongated to bind a target DNA sequence and substrate. This binary structure self-assembles upon hybridizing to a target analyte and the catalytic core is reformed, allowing for cleavage of a substrate to render a signal. The sensors were test against two targets of interest, TWIST-86 and AMELY. TWIST-86 is a target of interest in breast cancer research because it contributes to hormone resistance. AMELY is a marker for sex identification and is part of the Amelogenin gene that codes for tooth enamel. These targets were chosen to show the broad application of this type of sensor. Both sensors were also tested at two different temperatures, 30^{o}C and 55^{o}C, to compare their versatility and stability. Comparing CMB with BiDz, under optimal conditions for a deoxyribozyme sensor, showed that both sensors have detection limits in the picomolar range. The lowest limit of detection was reached by BiDz with 8 pM, and the CMB reached 59.5 pM, when detecting the

AMELY sequence. For the TWIST analyte, the lowest detection limit was 26.2 pM by BiDz, and 31 pM by CMB.

Typically, molecular beacons can only detect 2 nucleotide substitutions, but being able to distinguish between one base pair substitutions is highly advantageous, especially when investigating SNPs. The binary element of BiDz allows for one probe to be short in length, making it more unstable when hybridizing to a mismatched sequence. CMB does not possess this ability, as shown in the direct comparison between the sensors. Selectivity was calculated by (1-Fmm/Fm), were Fmm is the mismatch sequence and Fm is the matched sequence. This was deemed as the differentiation factor (DF). A DF greater that 0.50 is acceptable selectivity for a sensor. BiDZ sensor for AMELY analyte possess a 0.89 DF at 55^{o}C, whereas CMB, under the same conditions, only had a 0.07 DF. For TWIST, at 30^{o}C, BiDZ obtained a 0.83 DF compared to 0.31 DF for CMB. No CMB sensor, under any conditions, was able to achieve a DF over 0.40.

When designing a deoxyribozyme sensor length of the sequence, secondary structure, and purification play major roles. The longer the sequence the higher the melting point, which means the sensor can function at higher temperatures. When designing the sensors to function at 55^{o}C instead of 30^{o}C 5-10 nucleotides must be added. Binary probe that function at 30^{o}C are shorter in sequence than ones that function at 55^{o}C. This step is a simple adjustment in design for BiDz. Unfortunately, a CMB sensor was unable to detect AMELY at 55^{o}C and always encountered leakage. A more difficult step is the stability of secondary structure, which can be used to predict if the sensor will bind the target sequence easily or if it will remain folded. In some cases, if the secondary structure is not stable enough, the sensor can cleave the substrate prematurely, no

analyte present. When this occurs an inhibitory fragment can be added to the structure to essentially inactivate the catalytic core. This inhibitory fragment can be lengthened to increase secondary structure if cleavage still occurs. For CMB, there must be a stable secondary structure since the catalytic core is fully intact. This step, however, does not apply to the binary design because the core is split in half. CMB_TWIST_A_30 was designed without an intentional inhibitory fragment, and leakage was seen. CMB_TWIST_30 then incorporated a 7 nucleotide long inhibitory fragment, and was able to detect the TWIST analyte. Yet, in a means to increase selectivity the analyte binding loop was shorten to 15 nucleotides from 40 nucleotides, and leakage reoccurred. For purification, standard desalting is acceptable for BiDz, but for CMB HPLC is needed. Unnecessary by products of synthesizing the sensor can somehow disrupt the stability of the sensor. HPLC purification is much more expensive than standard desalting. As seen by the multiple failed CMB sensors, design complexity, and extra cost, CMB design is not as straightforward as BiDz. Overall, BiDz proves, in a direct comparison, to be more advantageous than CMB, in terms of selectivity, design simplicity, and cost.

The superiority of the BiDz, in molecular diagnostics, can be used to improve the field of human sex determination when paired with an isothermal amplification technique. BiDz sensors were easily designed to detect two Amelogenin gene sequences specific for X and Y chromosomes. The Amelogenin gene, which codes for tooth enamel, differs in sequence and length between the sex chromosomes, and is a widely used marker for sexing. Other current markers are standard tandem repeats (STR) and sex determining region Y (SRY) on the Y chromosome. Molecular-based techniques are needed when only blood samples, bone fragments or juvenile remains are present. Typically, molecular-based sex identification is carried out by

PCR analysis and amplification of one or multiple markers. This type of analysis can take time and must be done in a laboratory. LAMP amplification and BiDZ detection only need a hot plate and a portable fluorimeter to determine the sex of unknown remains.

X and Y sensors were characterized by their detection limits and selectivity. The X sensor was able to detect AMELX at as a low as 38 pM after 3 hours of incubation at 55ºC and the Y sensor detect AMELY at 11 pM, under the same conditions. Low detection limits will allow this detection method to be broadly applied. For instance, it can be applied to ancient DNA analysis, which works with only miniscule amounts of DNA and needs molecular diagnostics when juvenile remains are present because even if they are intact, conventional metric analysis cannot be applied. In good practice, the sensors were tested against the non-specific or mismatched analyte, to assess selectivity. Using 1 nM of analyte for both sensors, the sensor showed no affinity for the mismatched analyte with no signal above the background.

For the sensors to be able to detected human DNA, the target sequence was amplified from DNA extracted from teeth, using isothermal loop-mediated amplification. Teeth were used because DNA can be well persevered by the enamel layer of the tooth and contamination is seen to a lesser degree. LAMP offers rapid amplification and produces large amounts of amplicon. LAMP successfully amplified the target sequence, AMELX and AMELY, within 15-60 minutes at 65ºC. The LAMP product was than analyzed by gel electrophoresis to confirm amplification. LAMP samples that were amplified for 30 minutes were tested with X and Y sensors. Even though contamination was seen in the negative controls containing no analyte, the BiDz sensors were able to differentiate between the background (NC) and the human DNA containing sample.

After 1 hour incubation at 55ºC, the target sequences were identified. For determination of sex, the Y sensor must yield s/b ratio of 1.5 for the human DNA containing sample over the negative control. The X sensor can serve as a control test to show confirmed the sample contains human DNA so no false analyses are produced. The X sensor showed 100% accuracy when detecting male and female DNA with the same s/b 1.5 parameter. The Y sensor exhibited 100% accuracy in female DNA with no significant signal above the background, but only 75% accuracy with male DNA. This method can be improved by redesigning the LAMP primers to possibly decrease non-specific amplification. Also, DNA extraction and purification can be optimized to lower any possible cross contamination or degradation of the DNA. With improved accuracy, combining a binary deoxyribozyme sensor with LAMP amplification can be a useful method for human sex determination.

Future work will consist of optimizing the sensor and LAMP conditions, as well as increasing the range of specimens used. The BiDZ sensor can be designed to function at 65^0C, the same temperature as amplification and could create a “one pot” method for sex determination. Also, using an exonuclease enzyme to digest one strand of the dsDNA could lead to a more sensitive method since ssDNA is easier to detect. For amplification, a limit of detection in terms of how much template is needed would be advantageous for ancient DNA studies. Typically very small amounts of ancient DNA is present and needs to be used responsibly. Once all conditions have to been optimized, multiple unidentified samples can be sexed with this method to determine the accuracy of using a binary deoxyribozyme sensor and LAMP within a larger range of samples.

Concluding points

CMB vs BiDZ

1. CMB and BiDZ demonstrate comparable detection limits of 34-160 pM at 30^{o}C after 1 hr reaction, which is about one order of magnitude better that that of traditional hybridization probes (e.g molecular beacon) reported in literature.

2. BiDZ surpasses CMB in selectivity by differentiating single nucleotide substitutions with higher differentiation factors both at 30 and 55^{o}C. This strongly suggest that BiDZ design is preferable over CMB if a differentiation of single base substitution in nucleic acids needs to be achieved.

3. The design of BiDz probe was more straightforward, while optimization of BiDZ-based assay was simpler than that for CMB. This makes a strong argument towards choosing BiDz if multicompetent sensor design is compatible with the assay conditions.

X and Y BiDZ sensors for human sex determination

1. DZ sensors for the detection of Amelogenin gene X or Y chromosome sequences were designed and optimized. The sensors demonstrated detection limits 38 pM for X sensor and 11 pM for Y sensor after 3 hours of assay with synthetic DNA analytes.

2. The DZ sensors demonstrated exceptional selectivity against AMELX and AMELY synthetic analytes. This property is important for accurate sex determination in human specimens

3. Rapid amplification using a new isothermal technique. 30 minute LAMP amplification of DNA originating from teeth; confirmed by gel electrophoresis. Amplification can be

carried out using a simple hot plate at 65ºC. This method is advantageous for onsite analysis since it is a time efficient and does not require instrumentation. Conventional amplification, PCR, requires a thermocycler and can take more than an hour for completion depending on the nature of the sample.

4. BiDz detects LAMP amplicon with 1 hour incubation at 55ºC and determines sex of human teeth. This is significant due to the double stranded and complex nature of the LAMP amplicons. LAMP amplifies the target sequence multiple times in various size fragments. Also, LAMP can produce high amounts of non-specific amplification because of the use of 5 primers. BiDz can determine the sex of a sample even in the presence of contamination. Since LAMP occurs rapidly, contamination can be difficult to circumvent, as seen in gel electrophoresis. The X and Y sensors were able to achieve s/b 1.5 for the DNA containing sample, allowing for sex determination.

5. Accuracy of detection needs to be improved. The X sensor, which serves as a control test for the confirmation of human DNA being present, was 100% accurate in determining the sex of human teeth. The Y sensor was only 75% accurate with 3 out of 4 LAMP samples being correctly identified. Optimization of amplification by redesigning the primers is needed to increase the amount of the targeted sequence, and decrease non-specific amplification.

REFERENCES

1. Joyce, G. F., Directed evolution of nucleic acid enzymes. *Annual review of biochemistry* **2004,** *73*, 791-836.

2. Achenbach, J. C.; Chiuman, W.; Cruz, R. P.; Li, Y., DNAzymes: from creation in vitro to application in vivo. *Current pharmaceutical biotechnology* **2004,** *5* (4), 321-36.

3. Kruger, K.; Grabowski, P. J.; Zaug, A. J.; Sands, J.; Gottschling, D. E.; Cech, T. R., Self-splicing RNA: autoexcision and autocyclization of the ribosomal RNA intervening sequence of Tetrahymena. *Cell* **1982,** *31* (1), 147-57.

4. Brown, A. K.; Li, J.; Pavot, C. M.; Lu, Y., A lead-dependent DNAzyme with a two-step mechanism. *Biochemistry* **2003,** *42* (23), 7152-61.

5. Kolpashchikov, D. M., A binary deoxyribozyme for nucleic acid analysis. *Chembiochem : a European journal of chemical biology* **2007,** *8* (17), 2039-42.

6. Bengtson, H. N.; Kolpashchikov, D. M., A differential fluorescent receptor for nucleic acid analysis. *Chembiochem : a European journal of chemical biology* **2014,** *15* (2), 228-31.

7. Xiao, Y.; Allen, E. C.; Silverman, S. K., Merely two mutations switch a DNA-hydrolyzing deoxyribozyme from heterobimetallic (Zn2+/Mn2+) to monometallic (Zn2+-only) behavior. *Chemical communications* **2011,** *47* (6), 1749-51.

8. Xiao, Y.; Chandra, M.; Silverman, S. K., Functional compromises among pH tolerance, site specificity, and sequence tolerance for a DNA-hydrolyzing deoxyribozyme. *Biochemistry* **2010,** *49* (44), 9630-7.

9. Gao, P.; Wei, J. M.; Li, P. Y.; Zhang, C. J.; Jian, W. C.; Zhang, Y. H.; Xing, A. Y.; Zhou, G. Y., Screening of deoxyribozyme with high reversal efficiency against multidrug resistance in breast carcinoma cells. *Journal of cellular and molecular medicine* **2011,** *15* (10), 2130-8.

10. Zhang, M.; Xu, S.; Minteer, S. D.; Baum, D. A., Investigation of a deoxyribozyme as a biofuel cell catalyst. *Journal of the American Chemical Society* **2011,** *133* (40), 15890-3.

11. Bartlett, J. M.; Stirling, D., A short history of the polymerase chain reaction. *Methods in molecular biology* **2003,** *226*, 3-6.

12. Rogers, T.; Saunders, S., Accuracy of sex determination using morphological traits of the human pelvis. *Journal of forensic sciences* **1994,** *39* (4), 1047-56.

13. Albanese, J., A metric method for sex determination using the hipbone and the femur. *Journal of forensic sciences* **2003,** *48* (2), 263-73.

14. Aye, V. O., Determination of sex by armbone dimensions. *Forensic science international* **2010,** *199* (1-3), 111 e1-3.

15. Bongiovanni, R.; Spradley, M. K., Estimating sex of the human skeleton based on metrics of the sternum. *Forensic science international* **2012,** *219* (1-3), 290 e1-7.

16. Dabbs, G., Sex determination using the scapula in New Kingdom skeletons from Tell El-Amarna. *Homo : internationale Zeitschrift fur die vergleichende Forschung am Menschen* **2010,** *61* (6), 413-20.

17. Francesquini Junior, L.; Francesquini, M. A.; De La Cruz, B. M.; Pereira, S. D.; Ambrosano, G. M.; Barbosa, C. M.; Daruge Junior, E.; Del Bel Cury, A. A.; Daruge, E., Identification of sex using cranial base measurements. *The Journal of forensic odonto-stomatology* **2007,** *25* (1), 7-11.

18. Green, R. E.; Krause, J.; Briggs, A. W.; Maricic, T.; Stenzel, U.; Kircher, M.; Patterson, N.; Li, H.; Zhai, W.; Fritz, M. H.; Hansen, N. F.; Durand, E. Y.; Malaspinas, A. S.; Jensen, J. D.; Marques-Bonet, T.; Alkan, C.; Prufer, K.; Meyer, M.; Burbano, H. A.; Good, J. M.; Schultz, R.; Aximu-Petri, A.; Butthof, A.; Hober, B.; Hoffner, B.; Siegemund, M.; Weihmann, A.; Nusbaum, C.; Lander, E. S.; Russ, C.; Novod, N.; Affourtit, J.; Egholm, M.; Verna, C.; Rudan, P.; Brajkovic, D.; Kucan, Z.; Gusic, I.; Doronichev, V. B.; Golovanova, L. V.; Lalueza-Fox, C.; de la Rasilla, M.; Fortea, J.; Rosas, A.; Schmitz, R. W.; Johnson, P. L.; Eichler, E. E.; Falush, D.; Birney, E.; Mullikin, J. C.; Slatkin, M.; Nielsen, R.; Kelso, J.; Lachmann, M.; Reich, D.; Paabo, S., A draft sequence of the Neandertal genome. *Science* **2010,** *328* (5979), 710-22.

19. Saunders, S. R.; Chan, A. H.; Kahlon, B.; Kluge, H. F.; FitzGerald, C. M., Sexual dimorphism of the dental tissues in human permanent mandibular canines and third premolars. *American journal of physical anthropology* **2007,** *133* (1), 735-40.

20. Scheuer, L., A blind test of mandibular morphology for sexing mandibles in the first few years of life. *American journal of physical anthropology* **2002,** *119* (2), 189-91.

21. Sutter, R. C., Nonmetric subadult skeletal sexing traits: I. A blind test of the accuracy of eight previously proposed methods using prehistoric known-sex mummies from northern Chile. *Journal of forensic sciences* **2003,** *48* (5), 927-35.

22. Vlak, D.; Roksandic, M.; Schillaci, M. A., Greater sciatic notch as a sex indicator in juveniles. *American journal of physical anthropology* **2008,** *137* (3), 309-15.

23. Cunha, E.; FIly, M. L.; Clisson, I.; Santos, A. L.; Silva, A. M.; Umbelino, C.; Cesar, P.; Corte-Real, A.; Crubezy, E.; Ludes, B., Children at the convent: Comparing historical data,

morphology and DNA extracted from ancient tissues for sex diagnosis at Santa Clara-a-Velha (Coimbra, Portugal). *J Archaeol Sci* **2000,** *27* (10), 949-952.

24. Loth, S. R.; Henneberg, M., Sexually dimorphic mandibular morphology in the first few years of life. *American journal of physical anthropology* **2001,** *115* (2), 179-86.

25. Palmirotta, R.; Verginelli, F.; Di Tota, G.; Battista, P.; Cama, A.; Caramiello, S.; Capasso, L.; Mariani-Costantini, R., Use of multiplex polymerase-chain-reaction assay in the sex typing of DNA extracted from archaeological bone. *Int J Osteoarchaeol* **1997,** *7* (6), 605-609.

26. Stone, A. C.; Milner, G. R.; Paabo, S.; Stoneking, M., Sex determination of ancient human skeletons using DNA. *American journal of physical anthropology* **1996,** *99* (2), 231-8.

27. Daskalaki, E.; Anderung, C.; Humphrey, L.; Gotherstrom, A., Further developments in molecular sex assignment: a blind test of 18th and 19th century human skeletons. *J Archaeol Sci* **2011,** *38* (6), 1326-1330.

28. Akane, A.; Shiono, H.; Matsubara, K.; Nakahori, Y.; Seki, S.; Nagafuchi, S.; Yamada, M.; Nakagome, Y., Sex identification of forensic specimens by polymerase chain reaction (PCR): two alternative methods. *Forensic science international* **1991,** *49* (1), 81-8.

29. Tozzo, P.; Giuliodori, A.; Corato, S.; Ponzano, E.; Rodriguez, D.; Caenazzo, L., Deletion of amelogenin Y-locus in forensics: literature revision and description of a novel method for sex confirmation. *Journal of forensic and legal medicine* **2013,** *20* (5), 387-91.

30. Schmidt, D.; Hummel, S.; Herrmann, B., Brief communication: multiplex X/Y-PCR improves sex identification in aDNA analysis. *American journal of physical anthropology* **2003,** *121* (4), 337-41.

31. Skoglund, P.; Stora, J.; Gotherstrom, A.; Jakobsson, M., Accurate sex identification of ancient human remains using DNA shotgun sequencing. *J Archaeol Sci* **2013,** *40* (12), 4477-4482.

32. Gibbon, V.; Paximadis, M.; Strkalj, G.; Ruff, P.; Penny, C., Novel methods of molecular sex identification from skeletal tissue using the amelogenin gene. *Forensic science international. Genetics* **2009,** *3* (2), 74-9.

33. Nakahori, Y.; Hamano, K.; Iwaya, M.; Nakagome, Y., Sex identification by polymerase chain reaction using X-Y homologous primer. *American journal of medical genetics* **1991,** *39* (4), 472-3.

34. Alvarez-Sandoval, B. A.; Manzanilla, L. R.; Montiel, R., Sex determination in highly fragmented human DNA by high-resolution melting (HRM) analysis. *PloS one* **2014,** *9* (8), e104629.

35. Andreasson, H.; Allen, M., Rapid quantification and sex determination of forensic evidence materials. *Journal of forensic sciences* **2003,** *48* (6), 1280-1287.

36. Varga, A.; James, D., Real-time RT-PCR and SYBR Green I melting curve analysis for the identification of Plum pox virus strains C, EA, and W: effect of amplicon size, melt rate, and dye translocation. *Journal of virological methods* **2006,** *132* (1-2), 146-53.

37. Bauer, C. M.; Niederstatter, H.; McGlynn, G.; Stadler, H.; Parson, W., Comparison of morphological and molecular genetic sex-typing on mediaeval human skeletal remains. *Forensic science international. Genetics* **2013,** *7* (6), 581-6.

38. (a) Zanoli, L. M.; Spoto, G., Isothermal amplification methods for the detection of nucleic acids in microfluidic devices. *Biosensors* **2013,** *3* (1), 18-43; (b) Notomi, T., Okayama,

H., Masubuchi, H., Loop-mediated isothermal amplification of DNA. *Nucleic acids research* **2000,** *28* (12).

39. Hall, B. D.; Spiegelman, S., Sequence complementarity of T2-DNA and T2-specific RNA. *Proceedings of the National Academy of Sciences of the United States of America* **1961,** *47*, 137-63.

40. (a) Navarro, E.; Serrano-Heras, G.; Castano, M. J.; Solera, J., Real-time PCR detection chemistry. *Clinica chimica acta; international journal of clinical chemistry* **2015,** *439*, 231-50; (b) Armitage, B. A., Imaging of RNA in live cells. *Current opinion in chemical biology* **2011,** *15* (6), 806-12; (c) Ostergaard, M. E.; Hrdlicka, P. J., Pyrene-functionalized oligonucleotides and locked nucleic acids (LNAs): tools for fundamental research, diagnostics, and nanotechnology. *Chemical Society reviews* **2011,** *40* (12), 5771-88; (d) Khakshoor, O.; Kool, E. T., Chemistry of nucleic acids: impacts in multiple fields. *Chemical communications* **2011,** *47* (25), 7018-24.

41. Gerasimova, Y. V.; Kolpashchikov, D. M., Nucleic acid detection using MNAzymes. *Chemistry & biology* **2010,** *17* (2), 104-6.

42. (a) Tyagi, S.; Kramer, F. R., Molecular beacons: probes that fluoresce upon hybridization. *Nature biotechnology* **1996,** *14* (3), 303-8; (b) Kolpashchikov, D. M., An elegant biosensor molecular beacon probe: challenges and recent solutions. *Scientifica* **2012,** *2012*, 928783; (c) Zheng, J.; Yang, R.; Shi, M.; Wu, C.; Fang, X.; Li, Y.; Li, J.; Tan, W., Rationally designed molecular beacons for bioanalytical and biomedical applications. *Chemical Society reviews* **2015,** *44* (10), 3036-55.

43. (a) Wang Q, C. L., Long Y, Tian H, Wu J, Molecular Beacons of Xeno-Nucleic Acid for Detecting Nucleic Acid. *Theranostics* **2013,** *3* (6), 13; (b) Junager, N. P.; Kongsted, J.;

Astakhova, K., Revealing Nucleic Acid Mutations Using Forster Resonance Energy Transfer-Based Probes. *Sensors* **2016,** *16* (8); (c) Kuang, T.; Chang, L.; Peng, X.; Hu, X.; Gallego-Perez, D., Molecular Beacon Nano-Sensors for Probing Living Cancer Cells. *Trends in biotechnology* **2017,** *35* (4), 347-359.

44. (a) Cardullo, R. A.; Agrawal, S.; Flores, C.; Zamecnik, P. C.; Wolf, D. E., Detection of nucleic acid hybridization by nonradiative fluorescence resonance energy transfer. *Proceedings of the National Academy of Sciences of the United States of America* **1988,** *85* (23), 8790-4; (b) Guo, J.; Ju, J.; Turro, N. J., Fluorescent hybridization probes for nucleic acid detection. *Analytical and bioanalytical chemistry* **2012,** *402* (10), 3115-25; (c) Warhurst, G.; Dunn, G.; Chadwick, P.; Blackwood, B.; McAuley, D.; Perkins, G. D.; McMullan, R.; Gates, S.; Bentley, A.; Young, D.; Carlson, G. L.; Dark, P., Rapid detection of health-care-associated bloodstream infection in critical care using multipathogen real-time polymerase chain reaction technology: a diagnostic accuracy study and systematic review. *Health technology assessment* **2015,** *19* (35), 1-142; (d) Didenko, V. V., DNA probes using fluorescence resonance energy transfer (FRET): designs and applications. *BioTechniques* **2001,** *31* (5), 1106-16, 1118, 1120-1.

45. Kolpashchikov, D. M., Binary probes for nucleic acid analysis. *Chemical reviews* **2010,** *110* (8), 4709-23.

46. Stojanovic, M. N.; de Prada, P.; Landry, D. W., Catalytic molecular beacons. *Chembiochem : a European journal of chemical biology* **2001,** *2* (6), 411-5.

47. (a) Silverman, S. K., Catalytic DNA: Scope, Applications, and Biochemistry of Deoxyribozymes. *Trends in biochemical sciences* **2016,** *41* (7), 595-609; (b) McManus, S. A.; Li, Y., The structural diversity of deoxyribozymes. *Molecules* **2010,** *15* (9), 6269-84; (c)

Emilsson, G. M.; Breaker, R. R., Deoxyribozymes: new activities and new applications. *Cellular and molecular life sciences : CMLS* **2002,** *59* (4), 596-607; (d) Ward, W. L.; Plakos, K.; DeRose, V. J., Nucleic acid catalysis: metals, nucleobases, and other cofactors. *Chemical reviews* **2014,** *114* (8), 4318-42.

48. (a) Lan, T.; Lu, Y., Metal ion-dependent DNAzymes and their applications as biosensors. *Metal ions in life sciences* **2012,** *10*, 217-48; (b) Schlosser, K.; Li, Y., Biologically inspired synthetic enzymes made from DNA. *Chemistry & biology* **2009,** *16* (3), 311-22.

49. (a) Sando, S.; Sasaki, T.; Kanatani, K.; Aoyama, Y., Amplified nucleic acid sensing using programmed self-cleaving DNAzyme. *Journal of the American Chemical Society* **2003,** *125* (51), 15720-1; (b) Tian, Y.; Mao, C., DNAzyme amplification of molecular beacon signal. *Talanta* **2005,** *67* (3), 532-7; (c) Song, P.; Xiang, Y.; Xing, H.; Zhou, Z.; Tong, A.; Lu, Y., Label-free catalytic and molecular beacon containing an abasic site for sensitive fluorescent detection of small inorganic and organic molecules. *Analytical chemistry* **2012,** *84* (6), 2916-22; (d) Xu, J.; Li, H.; Wu, Z. S.; Qian, J.; Xue, C.; Jia, L., Double-stem Hairpin Probe and Ultrasensitive Colorimetric Detection of Cancer-related Nucleic Acids. *Theranostics* **2016,** *6* (3), 318-27; (e) Fu, R.; Li, T.; Lee, S. S.; Park, H. G., DNAzyme molecular beacon probes for target-induced signal-amplifying colorimetric detection of nucleic acids. *Analytical chemistry* **2011,** *83* (2), 494-500; (f) Mokany, E.; Bone, S. M.; Young, P. E.; Doan, T. B.; Todd, A. V., MNAzymes, a versatile new class of nucleic acid enzymes that can function as biosensors and molecular switches. *Journal of the American Chemical Society* **2010,** *132* (3), 1051-9; (g) Gerasimova, Y. V.; Cornett, E.; Kolpashchikov, D. M., RNA-cleaving deoxyribozyme sensor for nucleic acid analysis: the limit of detection. *Chembiochem : a European journal of chemical biology* **2010,** *11*

(6), 811-7, 729; (h) Ruble, B. K.; Richards, J. L.; Cheung-Lau, J. C.; Dmochowski, I. J., Mismatch Discrimination and Efficient Photomodulation with Split 10-23 DNAzymes. *Inorganica chimica acta* **2012,** *380*, 386-391; (i) Zagorovsky, K.; Chan, W. C., A plasmonic DNAzyme strategy for point-of-care genetic detection of infectious pathogens. *Angewandte Chemie* **2013,** *52* (11), 3168-71; (j) Gerasimova, Y. V.; Kolpashchikov, D. M., Folding of 16S rRNA in a signal-producing structure for the detection of bacteria. *Angewandte Chemie* **2013,** *52* (40), 10586-8; (k) Gerasimova, Y. V.; Cornett, E. M.; Edwards, E.; Su, X.; Rohde, K. H.; Kolpashchikov, D. M., Deoxyribozyme cascade for visual detection of bacterial RNA. *Chembiochem : a European journal of chemical biology* **2013,** *14* (16), 2087-90; (l) Bone, S. M.; Hasick, N. J.; Lima, N. E.; Erskine, S. M.; Mokany, E.; Todd, A. V., DNA-only cascade: a universal tool for signal amplification, enhancing the detection of target analytes. *Analytical chemistry* **2014,** *86* (18), 9106-13; (m) Gerasimova, Y. V.; Yakovchuk, P.; Dedkova, L. M.; Hecht, S. M.; Kolpashchikov, D. M., Expedited quantification of mutant ribosomal RNA by binary deoxyribozyme (BiDz) sensors. *Rna* **2015,** *21* (10), 1834-43; (n) Zhang, L.; Zhu, J.; Li, T.; Wang, E., Bifunctional colorimetric oligonucleotide probe based on a G-quadruplex DNAzyme molecular beacon. *Analytical chemistry* **2011,** *83* (23), 8871-6; (o) Cox, A. J.; Bengtson, H. N.; Gerasimova, Y. V.; Rohde, K. H.; Kolpashchikov, D. M., DNA Antenna Tile-Associated Deoxyribozyme Sensor with Improved Sensitivity. *Chembiochem : a European journal of chemical biology* **2016,** *17* (21), 2038-2041; (p) Cox, A. J.; Bengtson, H. N.; Rohde, K. H.; Kolpashchikov, D. M., DNA nanotechnology for nucleic acid analysis: multifunctional molecular DNA machine for RNA detection. *Chemical communications* **2016,** *52* (99), 14318-14321.

50. Kobe, B.; Kemp, B. E., Active site-directed protein regulation. *Nature* **1999,** *402* (6760), 373-6.

51. Dollfus, H.; Kumaramanickavel, G.; Biswas, P.; Stoetzel, C.; Quillet, R.; Denton, M.; Maw, M.; Perrin-Schmitt, F., Identification of a new TWIST mutation (7p21) with variable eyelid manifestations supports locus homogeneity of BPES at 3q22. *Journal of medical genetics* **2001,** *38* (7), 470-2.

52. (a) Nakahori, Y.; Takenaka, O.; Nakagome, Y., A human X-Y homologous region encodes "amelogenin". *Genomics* **1991,** *9* (2), 264-9; (b) Frances, F.; Portoles, O.; Gonzalez, J. I.; Coltell, O.; Verdu, F.; Castello, A.; Corella, D., Amelogenin test: From forensics to quality control in clinical and biochemical genomics. *Clinica chimica acta; international journal of clinical chemistry* **2007,** *386* (1-2), 53-6.

53. (a) Santoro, S. W.; Joyce, G. F., A general purpose RNA-cleaving DNA enzyme. *Proceedings of the National Academy of Sciences of the United States of America* **1997,** *94* (9), 4262-6; (b) Santoro, S. W.; Joyce, G. F., Mechanism and utility of an RNA-cleaving DNA enzyme. *Biochemistry* **1998,** *37* (38), 13330-42.

54. (a) Henihan, G.; Schulze, H.; Corrigan, D. K.; Giraud, G.; Terry, J. G.; Hardie, A.; Campbell, C. J.; Walton, A. J.; Crain, J.; Pethig, R.; Templeton, K. E.; Mount, A. R.; Bachmann, T. T., Label- and amplification-free electrochemical detection of bacterial ribosomal RNA. *Biosensors & bioelectronics* **2016,** *81*, 487-94; (b) Alladin-Mustan, B. S.; Mitran, C. J.; Gibbs-Davis, J. M., Achieving room temperature DNA amplification by dialling in destabilization. *Chemical communications* **2015,** *51* (44), 9101-4; (c) Du, T. E.; Wang, Y.; Zhang, Y.; Zhang, T.; Mao, X., A novel adenosine-based molecular beacon probe for room temperature nucleic acid

rapid detection in cotton thread device. *Analytica chimica acta* **2015,** *861*, 69-73; (d) Lingam, S.; Beta, M.; Dendukuri, D.; Krishnakumar, S., A focus on microfluidics and nanotechnology approaches for the ultra sensitive detection of microRNA. *MicroRNA* **2014,** *3* (1), 18-28.

55. Zuker, M., Mfold web server for nucleic acid folding and hybridization prediction. *Nucleic acids research* **2003,** *31* (13), 3406-15.

56. Bhadra, S.; Ellington, A. D., A Spinach molecular beacon triggered by strand displacement. *Rna* **2014,** *20* (8), 1183-94.

57. (a) Dark, P.; Blackwood, B.; Gates, S.; McAuley, D.; Perkins, G. D.; McMullan, R.; Wilson, C.; Graham, D.; Timms, K.; Warhurst, G., Accuracy of LightCycler((R)) SeptiFast for the detection and identification of pathogens in the blood of patients with suspected sepsis: a systematic review and meta-analysis. *Intensive care medicine* **2015,** *41* (1), 21-33; (b) Didenko, L. V., [Ultrastructural analysis as a method of studying bacteremia in infectious diseases]. *Vestnik Rossiiskoi akademii meditsinskikh nauk* **2001,** (11), 29-34; (c) Kolpashchikov, D. M., Binary malachite green aptamer for fluorescent detection of nucleic acids. *Journal of the American Chemical Society* **2005,** *127* (36), 12442-3; (d) Kolpashchikov, D. M., A binary DNA probe for highly specific nucleic Acid recognition. *Journal of the American Chemical Society* **2006,** *128* (32), 10625-8; (e) Kolpashchikov, D. M., Split DNA enzyme for visual single nucleotide polymorphism typing. *Journal of the American Chemical Society* **2008,** *130* (10), 2934-5; (f) Kolpashchikov, D. M.; Gerasimova, Y. V.; Khan, M. S., DNA nanotechnology for nucleic acid analysis: DX motif-based sensor. *Chembiochem : a European journal of chemical biology* **2011,** *12* (17), 2564-7; (g) Cornett, E. M.; O'Steen, M. R.; Kolpashchikov, D. M.,

Operating Cooperatively (OC) sensor for highly specific recognition of nucleic acids. *PloS one* **2013,** *8* (2), e55919.

58. Nogami, H.; Tsutsumi, H.; Komuro, T.; Mukoyama, R., Rapid and simple sex determination method from dental pulp by loop-mediated isothermal amplification. *Forensic science international. Genetics* **2008,** *2* (4), 349-53.

59. Stancescu, M.; Fedotova, T. A.; Hooyberghs, J.; Balaeff, A.; Kolpashchikov, D. M., Nonequilibrium Hybridization Enables Discrimination of a Point Mutation within 5-40 degrees C. *Journal of the American Chemical Society* **2016**.